

**Politecnico di Torino
&
State University of Unicamp Campinas**



UNICAMP

**Masters in Mechanical Engineering
Experimental study on combined window/solar collector for passive
thermal comfort and water heating**

**Supervisor in Unicampi, Campinas
Prof. Kamal A.R Ismail
Department of Energy Campinas, Brazil**

**Supervisor in Politecnico the Torino
Prof. Massimo Santarelli
Department of Energy Torino, Italy**

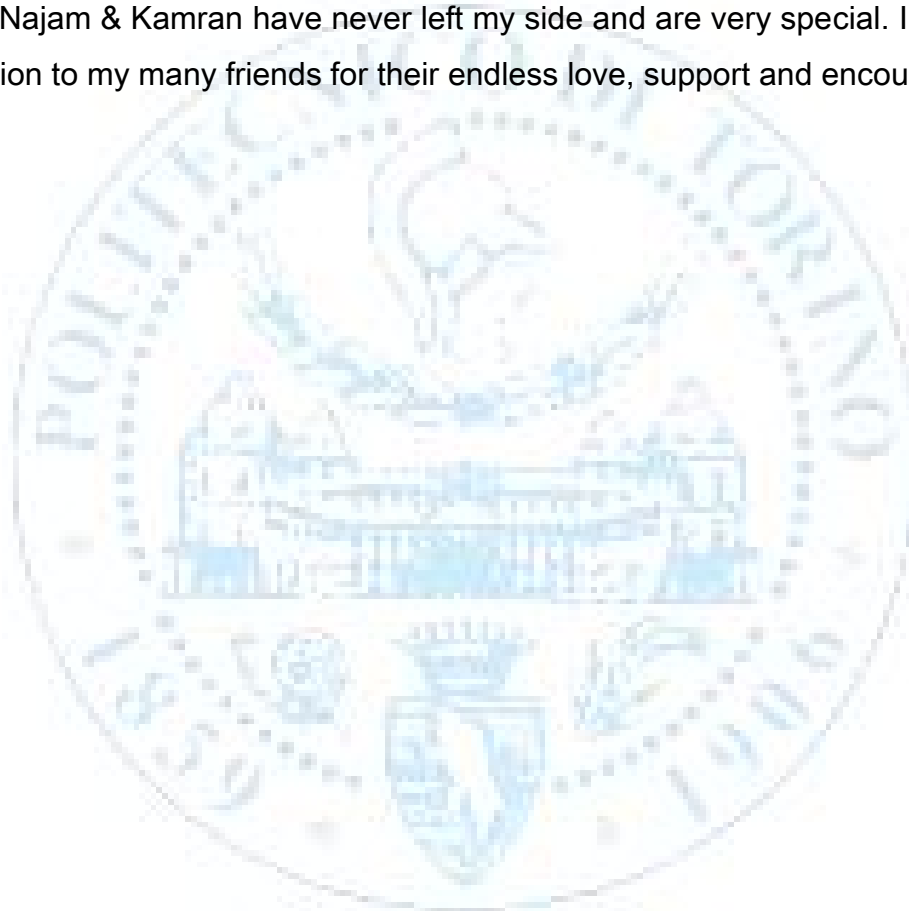
**By
Zeeshan Ali
S211121**

Dedication

There are a number of people without whom this thesis might not have been written, and to whom I am greatly indebted. I dedicate my dissertation work to my family and many friends. A special feeling of gratitude to my loving parents, Muhammad Anwar & Rukhsana kaussar whose words of encouragement and push for tenacity ring in my ears.

I dedicate this work and give special thanks to Muhammad Toseef Akram for being there for me throughout the entire program.

My brothers Najam & Kamran have never left my side and are very special. I also dedicate this dissertation to my many friends for their endless love, support and encouragement.



Acknowledgments

First and foremost, I must acknowledge my limitless thanks to Allah, the Ever-Magnificent; the Ever-Thankful, for his help and bless. I am totally sure that this work would have never become truth, without his guidance.

I owe a deep debt of gratitude to the universities Politecnico di Torino and Unicamp Campinas, Brazil for giving me an opportunity to complete this work.

I am grateful to my supervisor **Prof. Kamal A.R Ismail** who has been always generous during all phases of the research. I appreciate his vast knowledge and skills in many areas.

I would like to take this opportunity to say warm thanks to all my beloved friends, who have been so supportive along the way of doing my thesis.

Last but not least, deepest thanks go to all people who took part in making this thesis real. Not least of all, I owe so much to my whole family for their undying support, their unwavering belief that I can achieve so much. Unfortunately, I cannot thank everyone by name because it would take a lifetime but, I just want you all to know that you count so much. Had it not been for all your prayers and benedictions, were it not for your sincere love and help, I would never have completed this thesis. So thank you all.

Abstract

Thermal comfort and water heating in buildings are two services which consume a lot of electric energy. Windows are essential esthetic elements in a building permitting natural illumination and visual contact with the external ambient. They are responsible for the big thermal load and degradation of the room interior due to UV radiation. Hot water is equally energy consuming service necessary for domestic and commercial sanitary activities. To reduce energy consumption and emissions while keeping passive thermal comfort and supply of hot water for general use, a novel window that combines the function as a window and also as a solar collector for hot water is proposed. This window can also be used as skylight element for natural internal illumination. The window is composed of double glass separated by a gap where water is allowed to flow under a head. A radiation reflecting film is fixed on inner surface of the second glass sheet. The combined window/solar collector were tested under real open air conditions at different angles of inclinations ranging from nearly 0° to 90° . The results indicate a thermal efficiency varying from 45% to 67% and hot water volume of 47(L) at final temperature of 57°C for collector area of $0.5358(\text{m}^2)$. Also it was found that, at small inclination angles the collector performance was also good confirming its suitability as an element for skylight.

Keywords.

Thermal comfort, solar collector, passive comfort, combined window/solar collector, free hot water

**EXPERIMENTAL STUDY ON COMBINED WINDOW / SOLAR COLLECTOR
FOR PASSIVE THERMAL COMFORT AND WATER HEATING**

Contents

1	Introduction	11
2	Evolution in window and glass	13
2.1	window history	13
2.2	Glass	19
2.3	Modern glass	19
2.4	Double glazing	20
2.4.1	Air sealed cavity	20
2.4.2	Gas filled design	20
2.4.3	Airflow windows	21
2.5	Glass properties	21
2.5.1	Tinted glazing	21
2.5.2	Reflective glazing	22
2.5.3	Low emissivity	22
3	Literature reviews	22
3.1	Solar radiation	22
3.2	Thermal solar energy scenarios	23
3.3	Thermal solar energy for water heating	23
3.4	Residential solar water heating in Brazil	27
3.5	Spectral composition of solar radiation	29
4	How window influence comfort	30
4.1	Short wave radiation	32
4.2	Long wave radiation	33
4.3	Radiant asymmetry from windows	33
4.4	3M window film	35
4.4.1	Improving energy efficiency	36
4.4.2	Comfortable working environment	36
4.4.3	Safe and more secure	36
4.4.4	Protection from the sun	37
4.4.5	Creating privacy	37
4.5	Film to glass risk assessment chart	37
5	Solar collectors	38

5.1	Types of solar collector	40
5.1.1	Tank type collector	40
5.1.2	Pool collector	41
5.1.3	Flat plate collector	41
5.1.4	Evacuated tube collector	43
5.1.5	Concentrating collector	45
6	Thermal analysis or Heat balance	47
6.1	Energy balance of the collector	47
6.2	Heat removal factor	47
6.3	Absorbed solar radiation	49
7	Heat losses	49
7.1	Window losses	49
7.2	collector overall heat losses coefficient	51
7.2.1	Top loss coefficient	51
7.2.2	Energy loss through the bottom of the collector	52
7.2.3	Edge losses	52
7.2.4	Duct and pipe loss factors	52
8	Heat losses reduce	54
8.1	Optimization of glazing	54
8.1.1	Multi-Layer glazing windows	54
8.1.2	Vacuum glazing	55
8.1.3	Basic fabrication	56
8.1.4	Gas filled glazing	57
9	Solar collector for passive thermal comfort and water heating	59
9.1	Experimental set-up	59
9.2	Test procedure	61
9.3	Theoretical analysis	62
10	Results and discussion	63
10.1	Variation of ambient temperature and wind speed with time.....	63
10.2	Obtained results at 90°.....	64
10.2.1	Radiations at 90°.....	64
10.2.2	Variation of outlet and inlet temperature with respect to time.....	65
10.3	Obtained results at 0°.....	65
10.3.1	Radiations at 0°.....	65

10.3.2 Variation of outlet and inlet temperature with respect to time.....	66
10.4 Obtained results at 45°	66
10.4.1 Solar radiations at 45°	66
10.4.2 Variation of outlet and inlet temperature with respect to angles.....	67
10.4.3 Useful heat gain at 45°	68
11 Conclusion	69
12 References	70



List of figures

Figure 1 Energy flow-paths within water-flow glazing system	13
Figure 2 Example of an early timber window	14
Figure 3 Leaded casement with stay	14
Figure 4 Larger mullioned subdivided window	15
Figure 5 Cross casement	15
Figure 6 Molding	16
Figure 7 Exposed sash box	17
Figure 8 Recessed sash box	18
Figure 9 Gothic style venetian sash window	18
Figure 10 Concealed sash box	19
Figure 11 Average hourly demand of electric energy per sector in Brazil	24
Figure 12 Installed capacity of solar collectors for water heating	25
Figure 13 Location of the cities for which the Typical Meteorological Year (TMY)	27
Figure 14 Percentile electric energy savings of a typical residential heating system in Brazil.....	28
Figure 15 Yearly electric energy savings of a typical residential heating system in Brazil.	29
Figure 16 Spectral composition of solar radiation	30
Figure 17 Window impacts on thermal comfort: solar radiation, long-wave radiation, convective drafts	31
Figure 18 Yearly variations in the “solar constant	35
Figure 19 3M window film	35
Figure 20 Conversion of solar radiation to other energy forms	38
Figure 21 Number of covers of solar collector	39
Figure 22 Equipment ratio of the collector	40
Figure 23 tank type collector	40
Figure 24 sketch of a pool collector	41
Figure 25 sketch of the tubes of a pool collector	41
Figure 26 Flat plate collector	42
Figure 27 Classification of flat-plate solar collectors	42
Figure 28 Evacuated tube collectors	43
Figure 29 Classification of evacuated solar collector	44

Figure 30 concentrating collector	45
Figure 31 Schematic of the sun at a distance R from a concentrator	46
Figure 32 Classification of concentrators	47
Figure 33 Plume for a cold surface	49
Figure 34 fluid temperature distribution	53
Figure 35 Schematic of vacuum glazing	57
Figure 36 the gas filled window sample	58
Figure 37 The relation between gap width and the U-value of <i>CO2</i> as media	58
Figure 38 The relation between gap width and the U-value of <i>SF6</i> as media	59
Figure 39(a) Experimental setup	59
Figure 39(b) Schematic diagram of double glass window/Solar collector as a water heating device	60
Figure 40 Variation of ambient temperature and wind speed with time.....	64
Figure 41 Variation of solar radiations during experimentation hours at 90°.....	65
Figure 42 Variation of hot water outlet temperatures during experimentation hours at 90°.....	65
Figure 43 Variation of solar radiation during experimentation hours at 0°.....	66
Figure 44 Variation of outlet and inlet temperature during experimentation at 0°.....	66
Figure 45 Variation of solar radiations during experimentation hours at 45°.....	67
Figure 46 Variation of temperature of different angles.....	67
Figure 47 Variation of heat gain at different angles.....	68
Figure 48 Variation of thermal efficiency at different angles.....	68

List of table

Table 1 Energy performance at center of glass of double-glazed vertical windows with 5.7 mm glass panes	20
Table 2 Energy performance at center of glass of 5.7-mm-thick single-pane vertical windows	21
Table 3 Cities for which the "Typical Meteorological Year" (TMY) was generated	26
Table 4 these recommendation are based on solar specifications representing film mounted on 1/8" (3mm) clear glass	37
Table 5 Classification of solar collectors according to concentration degree	39
Table 6 Classification of collectors according to heat transfer medium	43
Table 7 U-value of different glazing layer	55
Table 8 Technical specification of the components and instruments	61
Table 9 presents the accuracy of various measuring devices used in the experiment.....	62



1. Introduction

Energy is one of the fundamental and essential requirements of living beings. Since the conventional energy resources are fast depleting and their cost is increasing, it is a prime concern of human being to save energy. Most of the power is obtained by the use of fossil fuels, (like coal, oil, gas etc.) which are not environmental friendly and emit an excessive amount of carbon dioxide and other pollutants that in turn cause global warming and greenhouse effects. The main solution to this problem is to effectively make use of the renewable energy sources available around us. Renewable energy is commonly defined as energy obtained from replenished natural resources such as solar energy, wind energy, tidal energy and wave's energy etc. Solar energy is one of the best and cleanest energy resources. The use of solar energy is not only beneficial to protect the natural environment of our world, also easily attainable, most economic and effective as compared to other energy resources.

Recently, integration of renewable energy system with architectural design has drawn the focus of researchers to make the building structure thermally efficient. (Directive 2010/31/EU, 2010). Precisely, windows are the major element responsible for building energy inefficiencies, due to the thermal loss or gain. Recent estimates depict that windows contribute 35% to 40% to the total building energy costs (U.S. Department of Energy (Ed.), 2009). The transmission index of a clear glass is about 90% which indicates that almost all the solar radiations can pass through it, which in turn are converted to heat when absorbed by internal ambient and are responsible for degradation of the room interior. Yet windows are obviously a necessary element of architecture, and architectural trends seem to show increasing usage of glass in building facades, which increases the problem further. Modern fenestration systems have been developed to improve building efficiency, cost adequacy and thermal comfort (Corgnati et al. 2007) because windows, without any doubt, are essential feature of an architectural design. The use of solar thermal collectors placed in certain parts of the building envelope has been suggested in order to resolve this concern (Hestnes, 1999).

In order to fulfil the increasing sustainability and conservation demands, window technology is going under rapid evolution. In recent years, a number of innovations in design and material have given new perspectives to window glazing. Literature review shows that considerable efforts had been invested in research and development of window technology. Some glass window concepts have been investigated by using alternative

filling materials such as silica aerogel by (Einarsrud et al. 1993), use of phase change materials (PCM) by (Ismail and Henríquez, 2002). Arasteh et al., (2008) have proposed the use of thin plastic films as non-structural center panes in order to improve efficiency yet maintaining overall window width, mass, and visual transmittance. Etzion and Erell (2000) described a novel ventilated reversible glazing system to minimize the transmission of radiant energy through windows. Their glazing system was designed in such a way that it was capable to overcome glare and radiation damage to interior furnishings, yet causing no energy-efficiency reduction compare to a conventional window. Ismail and Salinas (2006) formulated simplified models for spectral radiation modeling by examining gases with strong infrared radiation absorption characteristics.

Ismail et al. (2008) compared the thermal efficiency of glass windows filled with absorbing gas with windows filled with phase change material (PCM). Fluid flow through the gap between the glass sheets of a double panel window can enhance the thermal efficiency of windows. Experimental work on ventilated windows has been reported by (Onur et al. 1996).

Chow et al. (2010) formulated a solar window for cooling-demand climate. Their paper describes an innovative concept of water-flow window and highlights the potential fields of application. The results indicate that this new design is able to supply hot water, as well as reduce air-conditioning load and increase thermal and visual comfort. Clarke et al. (2011). Tested a prototype of the water-flow glazing system, with a reflective coating at the inner pane. Their results show that the year-round space cooling load for a range of feed water flow rates can be reduced from 22% to 35%. Chow and Chunying (2013) presented a liquid-filled solar glazing design for water-flow. A water-flow window had been constructed at the front wall of an environmentally controlled test cell to keep track of its performance under full-scale operational building-like conditions. A comparative study was done in which different glazing types were used.

This paper proposes a novel combined window /solar collector for passive thermal comfort and water heating as a particular type of Transparent Solar Thermal Collector that has two glass sheets making up a chamber through which water can flow in a controlled way. The static head of the water circuit allows stream of water to flow within the gap between the two glass sheets. A radiation reflective film is provided at the inner glass sheet. This combined window/solar collector absorbs a part of the incident solar radiation, which is

then utilized to heat up the water flowing through the gap between two glass sheets. The energy flow-paths related to such a glazing system are shown in Figure.1.

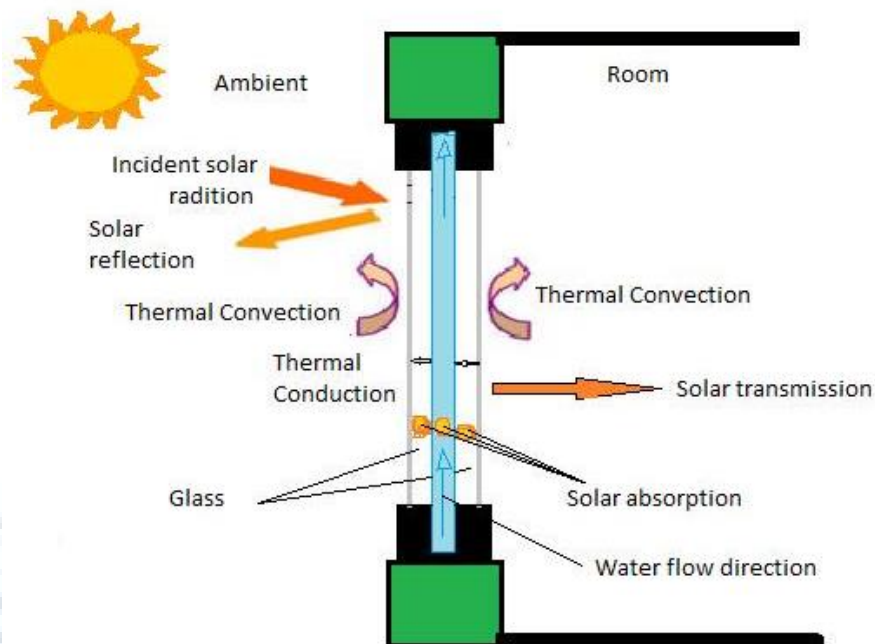


Figure 1 Energy flow-paths within water-flow glazing system

2. Evolution in Windows and glass

Windows are a building's most prominent feature because window design has evolved over the centuries windows can be invaluable in dating and in recognising later phases of alteration. Window design is closely related to the evolution of architectural styles, framing materials and, most importantly, to technological advances in the manufacturing of glass. The importance of windows is in their details:-

- Construction • Materials • Fittings • Mechanics • Glass

Window design reflects the status of the building and the social hierarchy within that building for example the difference between principal reception rooms and servants' rooms in basement or attic. Local style was usually far slower to respond to the latest fashion, and frequently developed in differing ways in differing regions.

2.1. History of window

Consequently localised types of window style contribute to creating a sense of local identity Pre 16th century windows were constructed from stone mullions or timber frames with unglazed openings. They could be closed by use of sliding or folding wooden shutters, oiled cloth, paper or even thin sheets of horn. Glazed windows were used only for the highest status buildings and were constructed of small panes of glass quarrels, (also

known as quarries), held together in a lattice of lead strips (comes). The lead was quite soft, so it was usually reinforced with iron bars either vertically (stanchions) or horizontally (saddle bars).



Figure 2 Example of an early timber window – Childswickham

Stone mullions were moulded on both inside and outside faces, usually with either a chamfer or cavetto moulding. Timber window frames were usually oak with pegged mortice and tenon joints and similarly moulded in imitation of more expensive stone.



Figure 3 Leaded casement with stay - Childswickham

Tudor stability and prosperity was reflected in window size. The much larger windows were subdivided into smaller openings (lights). Both stone and timber had vertical bars (mullions) and horizontal bars (transoms).



Figure 4 Larger mullioned subdivided windows – Offenham

A wrought-iron frame set into the mullions with smaller opening frame (hinged casement) provided an opening window. It would be latched shut with an iron catch or held open with an iron stay. In opening lights leaded glazing would be attached to the casement, in fixed lights it would be set into the mullions. As glass became more available throughout the century windows in wealthy aristocratic households became even larger in a peculiarly English tradition. In contrast the Italian Renaissance influence in Europe resulted in window design conforming to classical ideals. In smaller houses glazing was still rare but becoming more common.

Windows began to conform to classical ideals at the accession of the House of Stuart in 1603 reflecting renewed contact with Europe and the classical influences of the Italian Renaissance. They became taller than they were wide, typically divided into four lights by a single mullion and transom often of masonry. As the century progressed they were increasingly constructed from timber and known as cross casement windows.



Figure 5 Cross casement - Elmley Castle

Glazing was placed almost flush with the external face of the window. Mouldings were confined to the internal face, usually ogee or reverse ogee. Frames were therefore less

conspicuous whilst the surface area of glass increased. Crown glass was introduced in 1674 leading to a form of cross-casement window that had larger panes of glass held in timber or iron glazing bars rather than thin small panes in a leaded lattice. This type of window was replaced in Britain by the newly invented sash. Many early timber frame buildings were adapted to the new fashion. With insertion of sash windows and sometimes a skin of brickwork or stone to cover the front of the timber frame. In the earliest type of sash window the top sash was fixed and the bottom sash slid upwards in a groove held open by means of pegs or metal catches. These existed well before the introduction in the latter part of the 17th century of the 'double hung' sliding sash window, where both upper and lower sashes hung on cords counter-balanced by hidden weights in a hollow part of the frame called the sash box. An intermediate 'single-hung' type provided the same counterweight mechanism. These sashes were always timber, usually oak or pine, with a grid of timber glazing bars to hold the glass. Glazing bars would be up to 35mm thick, often with a flat external face and an ovolo moulded internal face (the thickness was to support the thick and heavy glass), they would divide the windows into as many as 16 panes in the upper sash and twenty in the lower. The double hung sash has remained virtually unchanged for over 250 years though its position in the wall changed significantly. Less common is a sideways sliding type of window called a Yorkshire sash.

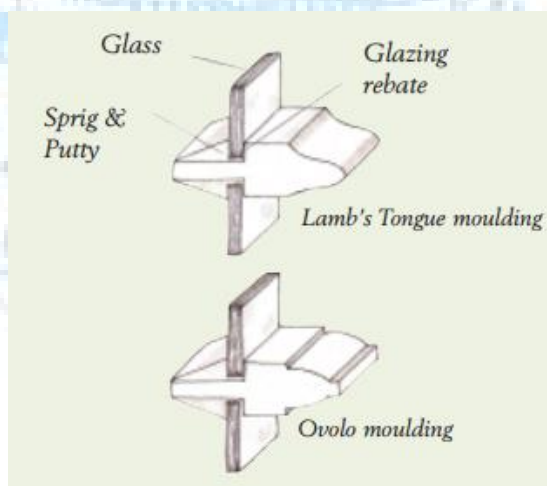


Figure 6 Moulding

At first the window was placed on the outer face of the wall, so the whole of the sash box was visible externally. After the Great Fire of London the exposed box was seen as a fire risk. In 1709 the London Building Act decreed that box sashes should be set back four inches from the face (recessed sash box). Originally this applied to Cities of London and Westminster spreading outwards with similar legislation being adopted by urban centres further afield.

A further London Building Act in 1774 required sash boxes to be placed behind the masonry (concealed-box sash). With the sash box out of sight the glazed area was larger. This Act was gradually adopted widely but the positioning of the box is not a reliable way of dating a building. Crown glass was very expensive which meant it was beyond the reach of most of the population so casement windows with leaded glazing remained popular throughout the 17th and much of the 18th centuries



Figure 7 Exposed sash box - Himbleton

At first the sash window altered little but as the century progressed design evolved and sash windows were made almost exclusively from Baltic Pine, glass got thinner, and the width of glazing bars slowly reduced. Internal mouldings were of the 'lamb's tongue' type. At the end of the century glazing bars on fine sashes were as little as 10mm wide. To make glazing bars or whole windows even more slender experiments were carried out in iron and copper. Introduction of plate glass in the 1770s led to further increase in pane size and reduced numbers of glazing bars, though cost meant this was only for the rich. There was some standardisation of windows for example the Georgian 'six over six' but there was also still a great deal of variation on grand and small houses with three over six and eight over eight though the very large sashes of the 17th century went out of fashion. Sashes became less expensive and by mid-century they could be found in humble homes, by the end of the century they were standard on even the smallest worker's dwelling. Early in the century they were painted pale colours but from the 1760s black was popular, particularly in ashlar stone or stuccoed houses. Greens, browns or graining effects were not uncommon. On some wealthy houses they were painted black and embellished with gold leaf.

Throughout the 18th century casement windows were replaced by sashes. Some survived in small rural dwellings and in late 18th to early 19th century 'cottage orne'. These windows increasingly had crown glass and timber glazing bars and casements, rather than the leaded glazing and wrought-iron opening casements of earlier windows.



Figure 8 Recessed sash box - Waterside, Evesham

Early in the 19th century patterns of glazing bars changed. Narrow 'margin' lights were common frequently filled with newly fashionable coloured glass. Sometimes glazing bars were curved into interlocking pointed Gothic style arches for 'Venetian' windows.



Figure 9 Gothic style venetian sash window – Pershore

Size of windows grew as many 18th century sashes had sills lowered to form access to balconies and sometimes were replaced by French windows.

Increased availability of plate glass meant that glazing bars could be reduced or removed completely. Improved methods of manufacture made glass less expensive from 1837. By mid century most windows had only one central glazing bar or none at all. 'Horns' were introduced to compensate for the increased weight of plate glass and lack of glazing bars.



Figure 10 Concealed sash box – Pershore

Victorian revivalist eclecticism in the 2nd half century of the 19th century brought a Gothic Revival with cast iron casements and imitation lead quarrel glazing with many small diamond or rectangular panes. There was some experimentation with setting plate glass in iron frames. These were not popular in houses being mainly used for conservatories, hot houses and industrial buildings. They were, however, popular on estate cottages. Later on in the century two new styles appeared; the 'Arts and Crafts' movement of genuine leaded lights, set in stone mullions or oak frames and the 'Queen Anne' movement with white painted small pane sash windows. These two became blurred and buildings often contained both elements and sometimes within the same window.

2.2. Glass

Old glass is of considerable historic and visual interest, contributing significantly to the character and appearance of old buildings. It has a rippling transparent vitality and greenish hue. Modern glass is featureless and uniform. Old cylinder and crown glass are irreplaceable. They are thin and easily broken and should not be removed from their original frames unless absolutely necessary.

2.3. Modern glass

Modern machine-made glass is generally not an appropriate alternative to hand made glass. Fine clear hand made cylinder glass is the only compatible glass

alternative today. Care must be taken in the selection of handmade glass as there are many types of cylinder glass. Cylinder glass produced for the art market makes poor substitutes for historic window glass. Handmade window glass can be obtained in the UK and there are some good imported glasses from Germany, France and Poland that are extremely close to old glasses that still survive.

2.4. Double Glazing

2.4.1. Air-sealed cavity

Using multiple panes of glass incorporated with air-sealed cavities makes it possible to increase the window insulation significantly. The presence of spacers holds the glass panes apart, accommodates thermal stress, and in addition, provides moisture barrier and gas-tight seal. Table 1 lists the energy performance of double-glazed windows that are built upon the single-glass panes introduced in Table 2. D1–D8 shows the results of adding a clear inner pane to each of S1–S8, with a 12.7 mm sealed air space and assuming the same steady-state environmental conditions.

Table 1 Energy performance at center of glass of double-glazed vertical windows with 5.7 mm glass panes (10.5 mm for PV laminated glass) and 12.7 mm cavity space (0.12 mm for vacuum space), under steady-state summer conditions: $G=1000 \text{ W/m}^2$; $y=601$; $T_a=33 \text{ }^\circ\text{C}$; $T_r=25 \text{ }^\circ\text{C}$; $h_o=22.7 \text{ W/m}^2 \text{ K}$; $h_i=8.29 \text{ W/m}^2 \text{ K}$

Case no.	Glass type	VT	U-factor	SHGC	Outer glass temp ($^\circ\text{C}$)	Inner glass temp ($^\circ\text{C}$)	Room heat gain (W/m^2)	Remark
D1	Clear+Air+Clear	0.793	3.035	0.596	37.1	34.9	380	
D2	Tinted+Air+Clear	0.476	3.037	0.388	44.7	36.0	256	
D3	Reflective on clear+Air+Clear	0.286	3.038	0.273	38.1	32.5	187	Reflective coating at surface 1
D4	Reflective on tinted+Air+Clear	0.110	3.038	0.216	40.0	32.7	153	Reflective coating at surface 1
D5	Low-e on clear+Air+Clear	0.706	1.625	0.303	41.7	30.8	194	Low-e coating at surface 2; ϵ
D6	Low-e on tinted+Air+Clear	0.450	1.636	0.209	48.8	30.5	138	Low-e coating at surface 2; $\epsilon=0.04$
D7	Low-e & reflective on clear+Air+Clear	0.274	1.625	0.121	50.6	29.7	85	Reflective +low-e coating at surface 2; $\epsilon=0.04$
D8	PV laminated glass+Air+Clear	0.095	2.700	0.177	47.3	35.2	127	Electricity generation=25.7W
D9	Clear+Argon+Clear	0.793	2.883	0.598	37.1	34.9	380	
D10	Low-e on clear+Argon+Low-e on clear	0.629	0.912	0.283	42.1	32.6	176	Low-e coatings at surfaces 2 and 3; $\epsilon=0.04$
D11	Low-e on clear+Vacuum+Low-e on clear	0.629	0.806	0.222	42.8	31.8	139	Low-e coatings at surfaces 2 and 3; $\epsilon=0.04$

It can be seen that the U-factor and SHGC values of the double clear glazing are reduced by 32–53% and 22–65%, respectively as compared to their single-pane counterparts; but the VT values remain reasonably high.

2.4.2. Gas-filled design

In summer, buoyant-induced air currents within the double glazing cavity carry absorbed heat to the window top along the outer pane and consequently, a cool pool developed at the bottom end of the inner pane [H.Manz et al. (2003)]. Filling the space with a less conductive and more viscous inert gas can minimize the scale of thermal

convection and conduction and thus improve the overall insulation characteristics. Manufacturers generally use argon or krypton as gas fills. These are non-toxic, nonreactive, clear, and odorless. The use of other suitable gas mixtures with strong infrared absorption are also studied [Ismail KAR, Salinas c.t. et al.(2008)].

2.4.3. Airflow windows

Double-pane windows may use cavity airflow as a means of improving heat recovery or reducing losses. Upward flow is typical in order to make full use of the thermal buoyancy effect. Methodology of assessment and comparison has been developed [Ismail KAR, Salinas c.t. et al.(2008)]. During the cooling season, an exhaust air window can extract air from the room to the outdoor space through vent openings. The driving force can be either the pressure differential (forced flow) or temperature differential (natural flow).

2.5. Glass properties

2.5.1. Tinted glazing

Tinted glass is specially formulated to cater for maximum absorption at part of the solar spectrum. Because of its high extinction coefficient, low transmittance and high absorptance, this is often called “absorptive” glass. The low transmittance reduces the quantity of transmitted daylight. Its primary use in window is therefore to reduce the effects of discomfort glare and solar transmission. All absorbed radiant energy is initially transformed into heat within the glass, thus raising the glass temperature. Table 2 lists the glass temperatures and the room heat gains for a selection of vertical single-glazed windows (all incorporated with 1 m 1 m glass pane) for ready reference.

Table 2 Energy performance at center of glass of 5.7-mm-thick single-pane vertical windows (10.5 mm for PV laminated glass) under steady-state summer conditions: $G=1000 \text{ W/m}^2$; $\gamma=601$; $T_a=33 \text{ }^\circ\text{C}$; $T_r=25 \text{ }^\circ\text{C}$; $h_o=22.7 \text{ W/m}^2 \text{ K}$; $h_i=8.29 \text{ W/m}^2 \text{ K}$

Case no.	Glass type	VT	U-factor	SHGC	Glass temp ($^\circ\text{C}$)	Room heat gain (W/m^2)	Remark
S1	Clear glass	0.888	6.010	0.777	34.0	465	
S2	Tinted glass	0.534	6.017	0.524	40.6	361	
S3	Reflective on clear glass	0.311	6.023	0.348	35.4	256	Reflective coating at surface 1
S4	Reflective on tinted glass	0.122	6.020	0.293	37.0	223	Reflective coating at surface 1
S5	Low-e on clear glass	0.792	2.406	0.467	40.1	241	Low-e coating at surface 2; $\epsilon=0.04$
S6	Low-e on tinted glass	0.506	2.406	0.423	46.6	189	Low-e coating at surface 2; $\epsilon=0.04$
S7	Low-e and reflective on clear glass	0.305	2.423	0.341	48.4	134	Reflective+low-e coating at surface 2; $\epsilon=0.043$
S8	PV laminated glass	0.106	5.701	0.280	43.5	213	Electricity generation=25.7 W
S9	Low-e on clear glass (reversed)	0.792	5.404	0.387	35.0	275	Low-e coating at surface 1; $\epsilon=0.04$
S10	Low-e on tinted glass (reversed)	0.506	5.404	0.301	38.1	229	Low-e coating at surface 1; $\epsilon=0.04$
S11	Low-e and reflective on clear glass (reversed)	0.305	5.708	0.210	39.4	179	Reflective+low-e coating at surface 1; $\epsilon=0.043$

Traditional tinted glazings, available in a range of colors like bronze and gray, allow a greater reduction in visible transmittance (VT) than in SHGC. They often face the practicality of how low the SHGC level has to be while maintaining an acceptable VT level. New developments, as described below, are then the spectrally selective glazings, with light blue/green tint having higher visible performance and favorably lower solar heat gain.

2.5.2. Reflective glazing

If achieving a higher reduction in solar gain is desirable, a reflective coating can be added to increase the reflectivity of the glass surface. In cases S3 and S4 of Table 2, there show 44.9% and 38.2% reductions in room heat gain, as compared to S1 clear glass and S2 tinted glass, respectively. The reflective coating, usually consisted of thin metallic or metal oxide layers, comes in various metallic colors such as bronze, silver, or gold.

2.5.3. Low-emissivity glazing

Low-emissivity (low-e) refers to a low emissivity over the longwavelength portion of the spectrum. Low-e coatings in colors of gold, silver or copper offer a range of solar control characteristics. A typical coating (of thickness around 0.1 mm) has three layers, i.e. a thin metal layer sandwiched between two dielectric layers. Its application is able to change the original longwave (143 mm) emissivity of around 0.9 to less than 0.1.

3. Literature reviews

3.1. Solar radiation

An assessment of the “magnitude” of solar radiation as an energy source will depend on the geographical location, including local conditions such as cloudiness, turbidity, etc. Its depend a number of features of the radiation flux at a horizontal plane were described, such as spectral distribution, direct and scattered parts, geographical variations, and dependence on time, from annual to diurnal variations at a given location.

For actual applications, it is often necessary to estimate the amount of radiation received by tilted or complexly shaped devices, and it is useful to look at relations which allow relevant information to be extracted from some basic measured quantities. For instance, radiation data often exist only for a horizontal plane, and a relation is therefore needed to predict the radiation flux on an arbitrarily inclined surface. In regions at high latitudes, directing solar devices towards the Equator at fairly high tilt angles actually gives an increase in incident energy relative to horizontally placed collectors.

3.2. THERMAL SOLAR ENERGY SCENARIOS

One of the main goals of SWERA was to provide reliable information regarding the solar resource (as well as wind), to be used by designers, financial analysts and legislators, due to the lack of reliable data.

This lack of good quality data made in many cases the uncertainties too high regarding the performance of systems, and consequently regarding the economic viability analysis of projects. As a consequence, the amount of investments in solar energy is reduced, once the risks would be, in many cases, at undesirable levels. The market for products using solar energy has been growing over the years. The economic feasibility of certain applications combined with the greater ecological awareness, along with a growing concern about the long-term impact of using conventional sources of energy, were the key factors for the growth of the market for equipment using solar energy.

One of the most important application of solar energy in Brazil is the one in which the solar energy is directly transformed into heat. Despite the high initial investment, the payback time is low, as will be further discussed in details. Thermal solar energy applications in other areas, such as the agro-industry, request for greater investments due to the low value added to production. For this reason, the technologies in use are generally not very sophisticated.

3.3. THERMAL SOLAR ENERGY FOR WATER HEATING

Thermal solar energy is one of the oldest applications of this energy source, where solar radiation is directly used to produce heat. The reasons that hinder the large-scale use of solar energy are the high variability, uncertainty, and discontinuity during the night and low energy density. In reason of that, the thermal use of solar energy is still small when compared to the combustion of firewood and fossil fuels, which have a much greater energy density.

Brazil has a particular characteristic that sets it apart from other countries regarding water heating for residential use. During the 1960s and 1970s, huge investments were made in the hydroelectric energy generation sector. Since economic growth did not go together with the growth in production during certain periods, the consumption of the exceeding electricity was encouraged, so electric showerheads became widely used in the country. Figure 11 shows the total and per sector demand of electricity in Brazil during the day.

By observing the curve that represents total demand, a pronounced peak can be seen during the early nighttime hours. This peak is reproduced in the residential consumption curve, which leads to the conclusion that this is the major responsible of the existence of

the "peak demand time" in electricity consumption. It is exactly during this peak demand time that the electric shower is most widely used, and therefore, its substitution may be considered as an efficient measure and rational use of electric energy in Brazil. Electric showerheads are high power equipment – above 4kW, reaching up to 7kW – with a low load factor, since they are used only a few minutes a day.

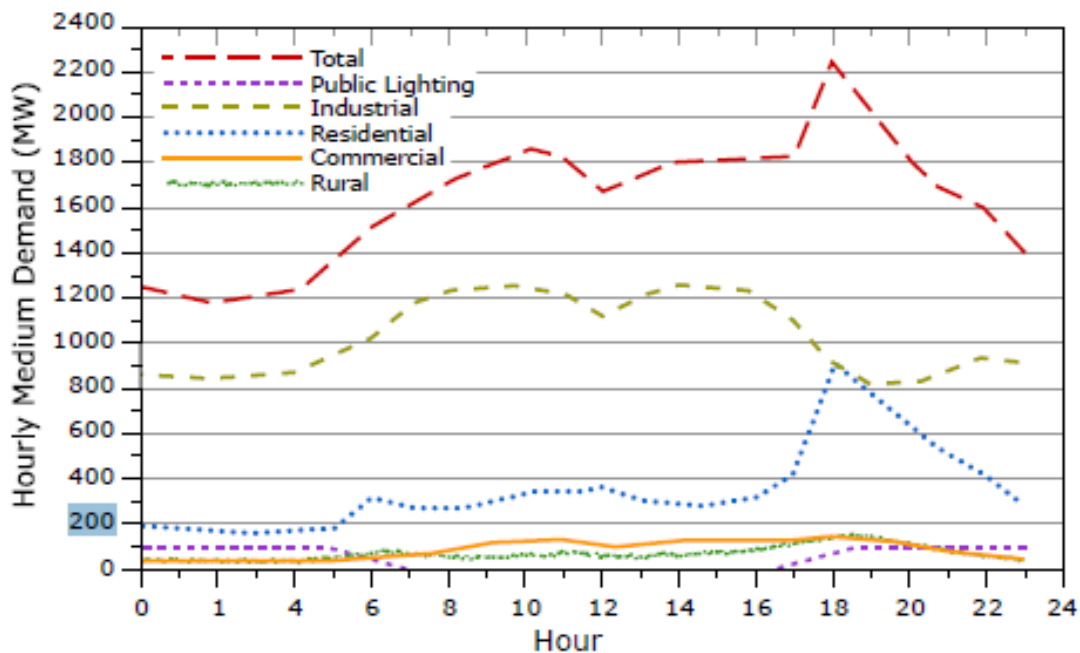


Figure 11. Average hourly demand of electric energy per sector in Brazil

Water heating is the most promising application of solar energy in Brazil. Currently, a fairly well developed market already exists for solar heating systems in Brazil, which has more than 2.2 million m² of thermal solar collectors for water heating installed. However, this area is small when compared to that of countries where the solar energy resource and the population are smaller, such as Germany (above 5.7 million m²), or Turkey (more than 7.2 million m²). The graph of Figure 12 shows the installed capacity in thermal Megawatts per group of 100,000 inhabitants in several countries. It can be observed that Brazil has a very low ratio, which indicates that a large market is still available in the country [Weiss, Bergmann fanning et al.(2004, 2006)].

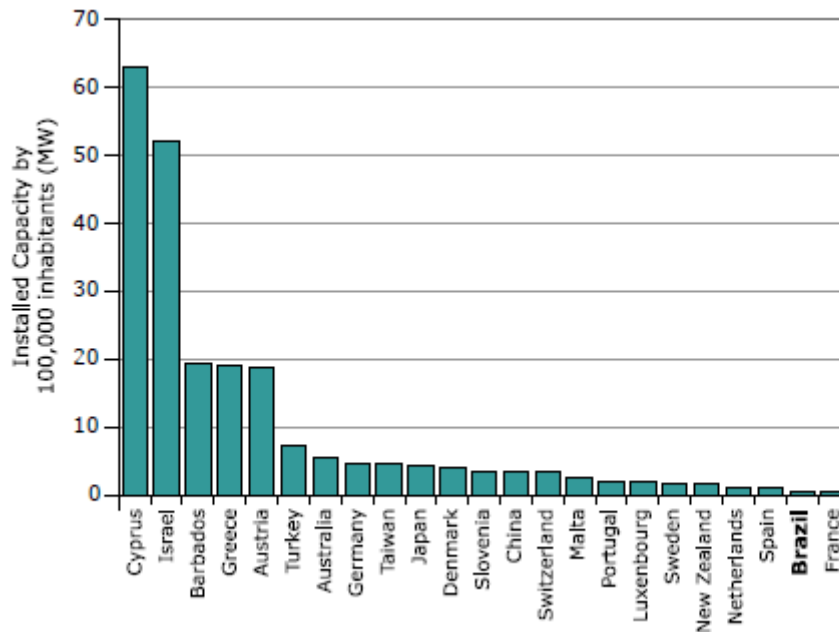


Figure 12 Installed capacity of solar collectors for water heating per group of 100,000 inhabitants in 2004.

There are several industries for solar heating systems in Brazil, which concentrate their production in flat plate solar collectors with glazing. Over the last years, some industries started producing plastic collectors without cover, used preferentially for heating swimming pools. Collectors with evacuated heat pipes are not yet manufactured in Brazil.

The low-cost home water solar heating system commonly used in Brazil consists of a flat plate collector and a storage tank. It operates by direct heating (no heat exchanger) and water circulation through a thermo-siphon. Generally, it does not consume electric energy, if some distance/heights are observed, otherwise a water circulation pump is necessary, and some energy is consumed.

The flat plate solar collectors consist of a black Copper absorber, a thermally insulated box and a front glazing. The hot water is stored in cylindrical insulated water tanks.

A labeling program, which started in 1998, headed by PROCEL and INMETRO, tests several characteristics of the collectors and tanks, and grants quality and efficiency labels. In 2007, the best labeled collectors have an efficiency of 77%.

The solar energy data generated during the SWERA project have a spatial resolution of 10km x 10km of the monthly averages for daily totals. More detailed simulations are necessary, which one SWERA project has also made available the typical meteorological years (TMY – available in the annexed CD-ROM) for the 20 Brazilian cities listed in Table 3. The choice of such cities prioritized the distribution throughout all Brazilian regions, as can be seen in Figure 13

Table 3 Cities for which the "Typical Meteorological Year" (TMY) was generated.

ID	City	State
1	Campo Grande	Mato Grosso do Sul
2	Curitiba	Paraná
3	Florianópolis	Santa Catarina
4	Fortaleza	Ceará
5	Recife	Pernambuco
6	Cuiabá	Mato Grosso
7	Petrolina	Pernambuco
8	Belo Horizonte	Minas Gerais
9	Porto Nacional	Tocantins
10	Boa Vista	Roraima
11	São Paulo	São Paulo
12	Brasília	Distrito Federal
13	Rio de Janeiro	Rio de Janeiro
14	Belém	Pará
15	Porto Velho	Roraima
16	Jacareacanga	Pará
17	Salvador	Bahia
18	Bom Jesus da Lapa	Bahia
19	Manaus	Amazonas
20	Santa Maria	Rio Grande do Sul

The most widely used scheme to simulate the performance of solar heating systems based on monthly solar radiation averages is the F-chart method [Klein,S.A.Beckman et al.(2000)]. By using the F-chart method together with SWERA data, it is possible to map the fraction of saved electricity. Based on this map, the detailed economic analysis and specific cases of practical interest were done.

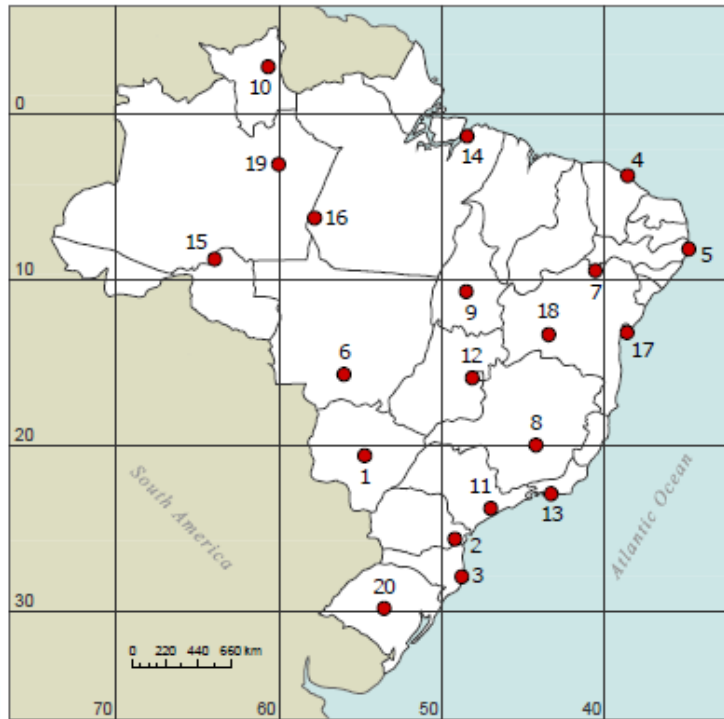


Figure 13 Location of the cities for which the Typical Meteorological Year (TMY) was generated during the SWERA project (numbered as per Table 3).

3.4. RESIDENTIAL SOLAR WATER HEATING IN BRAZIL

The most remarkable characteristic of the solar energy market in Brazil is that the main users there are higher income families. The reason for this is the high initial cost of a solar heating system when compared to the electric showerhead alternative. However, the solar water heating system is normally not considered in the design phase, but adapted to existing houses. As a result, normally the collectors are not installed at optimum orientation and tilt, so the area of collectors must be increased, and the systems become more expensive.

On the other hand, in high-income residences, a conventional electric or gas water heating system is normally already considered during the design phase. Therefore, hot water distribution plumbing is already existent, which consequently reduces the additional price of the solar heating system when it is adapted, in relation to the additional installation cost of the collection panels.

Additionally, in some important urban areas of Brazil, like Rio de Janeiro and Sao Paulo, the use of gas (Natural Gas or LPG) water heating systems is widespread. Since the cost of operation of these systems are very low (much lower than the electric water heating systems), there is little interest in installing solar heating systems.

For lower income residences, the most common option ends up being the electric showerhead, where no cost is required for hot water distribution, since the heating is done directly at the consumption point and, therefore, the costs of a solar heating system becomes even

more unfavorable. In order to partially solve this problem, some manufacturers produce compact systems, for smaller hot-water demands and with external hot water distribution.

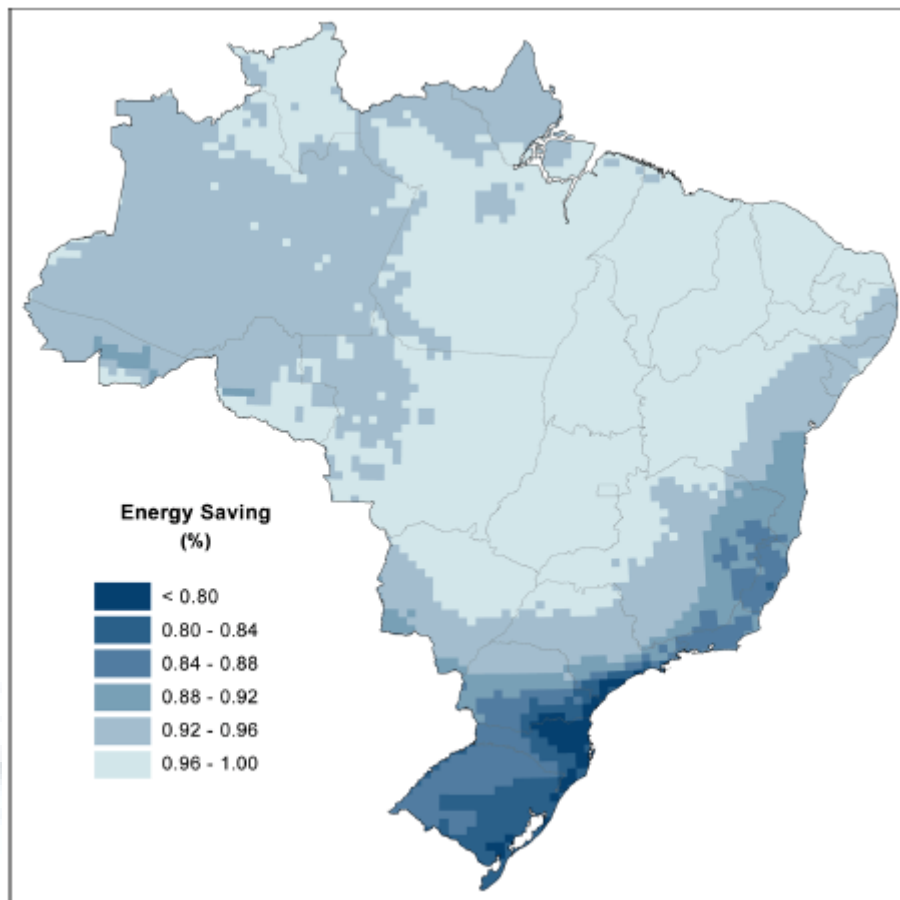


Figure 14 Percentile electric energy savings of a typical residential heating system in Brazil.

The map of Figure 14 shows the percentage of electric energy saved per one family, which needs around 300 liters of hot water per day. For this simulation, the performance characteristics of a flat-plate solar collector with a single glass cover of 60% efficiency, were adopted. Currently this is the standard configuration available in the Brazilian market. In order to calculate the heating needs, the required energy is assumed as a function of the monthly average temperature for each point on the map. The simulated system had 4m² of area and a water tank volume of to 300 liters.

The map of Figure 15 shows the energy produced per year considering the described system. It can be observed that despite the relative energy savings being higher at locations with warmer weather, the produced energy is not so different for the several Brazilian regions.

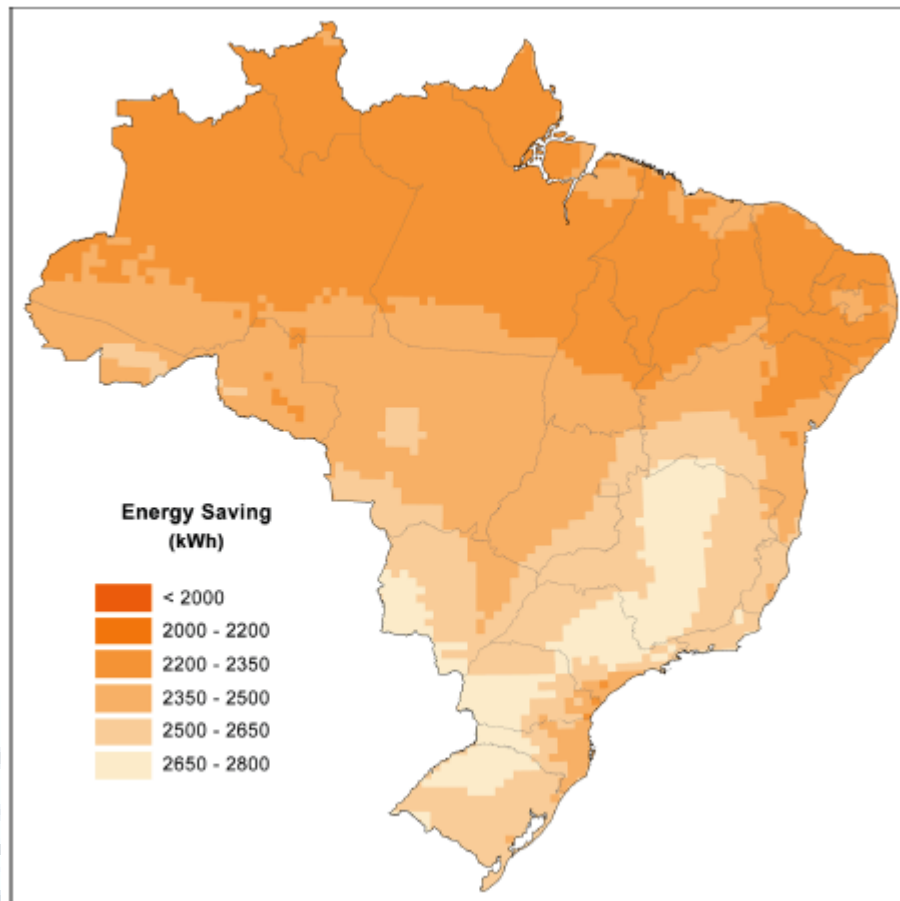


Figure 15 Yearly electric energy savings of a typical residential heating system in Brazil.

Bearing in mind the economical point of view, the payback time of this solar heating system is lower in regions with more favorable climate, but the quantity of saved energy may be greater in regions where the demand for water heating is larger once the system is correctly sized.

3.5. Spectral composition of solar radiation

Practically all of the radiation from the Sun received at the Earth originates in the photosphere, a thin layer surrounding the convective mantle of high. Figure 16 Variation in the solar radius as a function of time (bottom), together with selected milestones in the development on Earth, associated with the building-up of oxygen in the Earth's atmosphere (top). The rapid development of phytoplankton in the upper layers of the oceans at a relative oxygen concentration of 10^{-2} is associated with the formation of an ozone shield in the atmosphere, cutting down the ultraviolet part of the solar spectrum. When the oxygen level has reached 10^{-1} , the atmospheric ultraviolet absorption is strong enough to allow life on land.

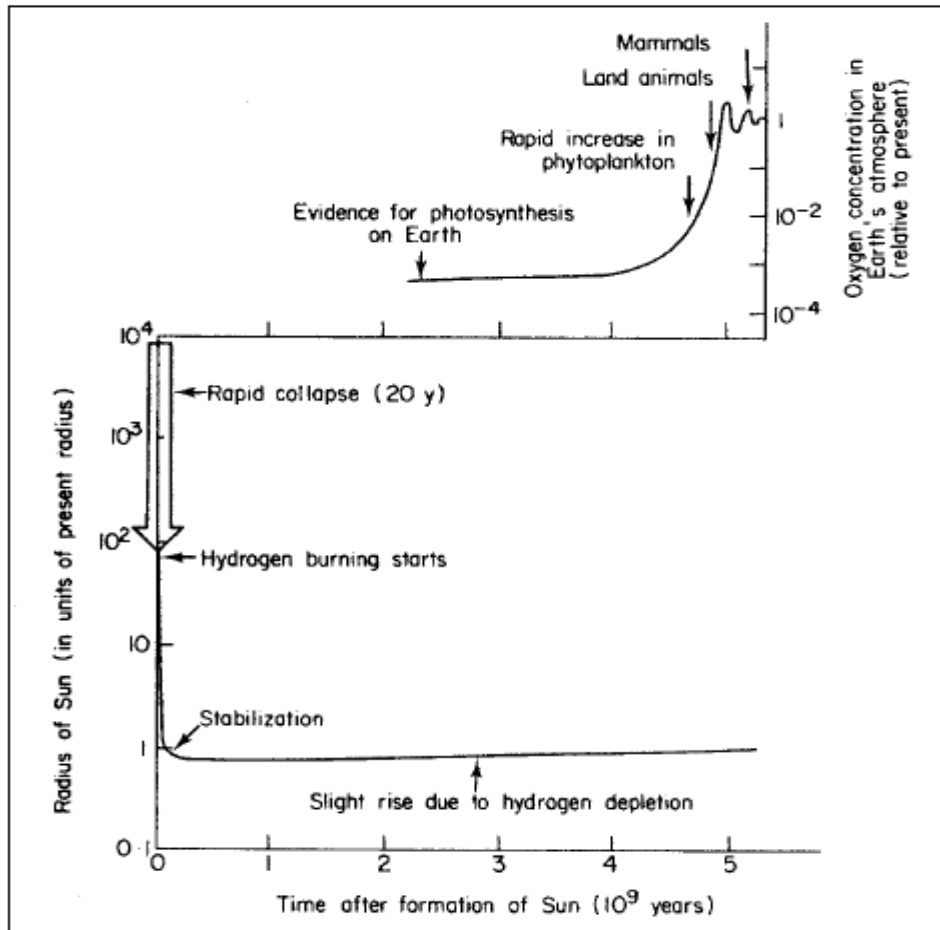


Figure 16 Spectral composition of solar radiation

The depth to which a terrestrial observer can see the Sun lies in the photosphere. Owing to the longer path-length in the absorptive region, the apparent brightness of the Sun decreases towards the edges. The photosphere consists of atoms of varying degree of ionization, plus free electrons.

A large number of scattering processes take place, leading to a spectrum similar to the Planck radiation (see section 2.A) for a black body in equilibrium with a temperature $T \approx 6000$ K. However, this is not quite so, partly because of sharp absorption lines corresponding to the transitions between different electron configurations in the atoms present (absorption lines of over 60 elements have been identified in the solar spectrum), partly because of the temperature variation through the photosphere, from around 8000 K near the convective zone to a minimum of 4300 K at the transition to the chromosphere. is in fair agreement with the Planck law for an assumed effective temperature $T_{eff} \approx 5762$ K, disregarding in this figure the narrow absorption lines in the spectrum.

4. HOW WINDOWS INFLUENCE COMFORT

A window influences thermal comfort in three ways (Figure 17):

- 1 long-wave radiation from the warm or cold interior glass surface

2 transmitted solar radiation

3 induced air motion (convective drafts) caused by a difference between the glass surface temperature and the adjacent air temperature

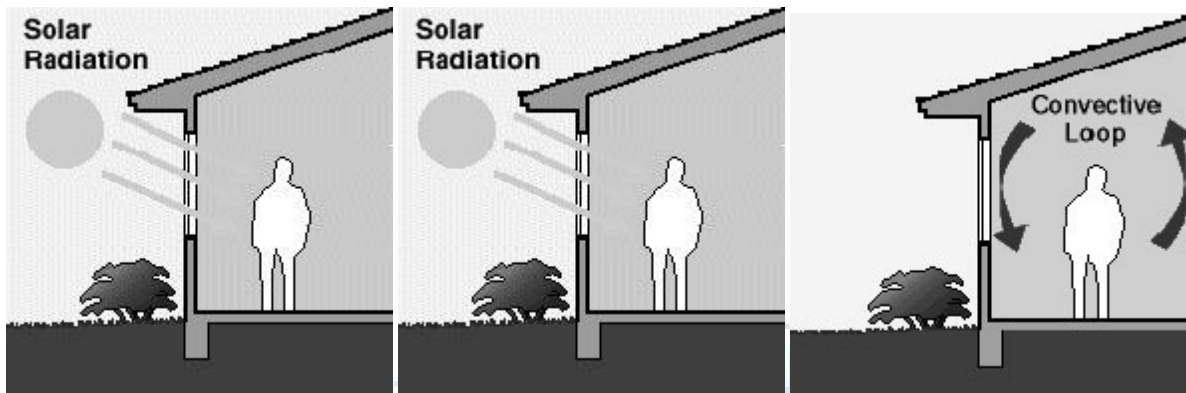


Figure 17 Window impacts on thermal comfort: solar radiation, long-wave radiation, convective drafts

Windows absorb and transmit a significant amount of solar radiation. Absorbed radiation influences the temperature of the glass; the inside surface of heat absorbing glass can routinely reach temperatures above 120°F (50°C) in summer conditions, raising MRT by as much as 15°F (8°C). Transmitted radiation often causes discomfort if it falls directly on the occupant. A person sitting near a window in direct solar radiation can experience heat gain equivalent to a 20°F (11°C) (Arens et al. 1986) rise in mean radiant temperature. These radiant heating and cooling effects act on the occupant's body asymmetrically, causing some parts of the body to be considerably cooler or warmer than a uniform model like MRT can describe.

Models need to consider the effect on local skin temperature in order to be sensitive to discomfort caused by windows. The inside surface temperature of a window is heavily influenced by exterior conditions and this temperature can significantly affect the radiant heat exchange between an occupant and the environment. If this heat exchange becomes greater than or less than the acceptable range, discomfort will result. Mean radiant temperature (MRT), defined as the uniform temperature of an imaginary enclosure in which the net radiation heat exchange between the occupant and the enclosure equals the net radiation heat exchange in the actual environment, is commonly used to simplify the characterization of the radiant environment. On a cold day the inside surface temperature can easily drop below 15°F (-9°C) for a clear single pane window and below 40°F (4°C) for a clear, double pane window. Although it is well understood how high-performance windows can reduce building energy consumption, a better understanding of how they affect comfort might lead to even greater savings.

4.1. SHORT-WAVE RADIATION

In a cold winter morning, direct sunlight on a person's body may be perceived as a pleasant presence. However, in summer daytime, solar radiation will almost certainly cause discomfort. Short-wave radiation causes thermal discomfort directly when it is absorbed by the body (or clothing) and indirectly by increasing the air and surface temperatures in a space. This latter impact is in theory moderated by the HVAC system. The HVAC system controls the air and surface temperatures in the space to compensate for solar gain. In practice, HVAC systems rarely achieve perfect control and as a result, solar gain often raises the operative temperature in perimeter zones.

Hausler and Berger (2002) found that when the air temperature is 22°C or above, direct solar radiation on the body causes discomfort. Schutrum et al. (1968) tested subject thermal sensation with solar radiation transmitted through a window whose glass temperature was separately controlled. When the glass temperature increased from 3°C to 48°C (room air temperature increased from 23.7 to 24.3°C) on a cloudy day, overall sensation elevated 1.1 units (from slightly cool to neutral, 7-point scale,). On a clear day with solar radiation on the body, the window temperature increased to 31.7°C and the overall sensation became 2.5 units warmer (from slightly cool to above slightly warm).

In summer, thermal comfort is mostly uncorrelated with U-value but is closely related to solar transmittance (Lyons et al. 1999). In fact, solar transmittance is the controlling factor with respect to the effect a particular glazing system will have on comfort. The T_{sol} of the glass determines the amount of solar gain that is transmitted into the space. Simulations show that replacing single 3mm clear glass ($T_{sol} = 0.83$) with double 3mm low-E glass ($T_{sol} = 0.53$) can reduce discomfort by more than half (Lyons et al. 1999). Sengupta et al. (2005) simulated comfort in a room and the results demonstrated that in summer daytime (780 W/m² solar radiation) the change from clear single glazing to clear double glazing did not significantly improve thermal comfort.

However, reducing the window size (from 40% to 20% glass-to-floor area ratio) significantly improved the comfortable floor area. Olesen & Parsons (2002) also discuss radiant discomfort and state that "direct solar radiation should be avoided in the occupied zone, by means of building design or solar shading devices".

Because solar transmittance is a major factor in determining comfort, a logical way to reduce solar radiation is to use glazing with a spectrally selective coating. Although glass temperature normally increases because of the higher solar absorptance of the film coating compared to normal glass, the reduction in solar transmittance can be more than 50%

(Arasteh et al. 1987, Alvarez et al. 1998, Karlson et al. 1988, Estrada-Gasca et al. 1993a and 1993b,

Ideally, a spectrally selective coating should have a small effect on visible transmittance, to preserve daylight and views, but will be near-opaque at other wavelengths. This is especially critical in the automobile industry where for safety reasons the visible transmittance must be 70% or above (Bohm et al. 2002, Nair and Nair 1991).

In buildings, ways of blocking solar radiation can also be achieved by applying shading elements, such as overhangs or curtains, (e.g. the Phoenix Public Library designed by William Bruder, and the Arup Campus designed by Arup Associates). They both used shading devices and the results are very good in terms of keeping both thermal and visual comfort).

4.2. LONG-WAVE RADIATION

Long-wave radiation from a warm or a cold window affects occupant comfort in two ways. First, it influences the overall radiative heat exchange between the body and the surroundings, affecting the body's heat balance and therefore comfort. Second, even when there is a neutral overall heat balance, local discomfort of one or more body part may result from asymmetric radiation fields near windows.

ASHRAE and ISO standards define a comfort zone for the body based on overall heat balance, however thermal neutrality is not the only condition to ensure thermal comfort. A person may feel thermally neutral for the body as a whole, but he may not be comfortable if one part of the body is warm and another cold. A further requirement to comfort is that no local warm or cold discomfort exists at any part of the body. Local discomfort can be caused by radiation temperature asymmetry such as a warm or cold window, ceiling, wall, or floor; excessive air motion (draft); or vertical air temperature stratification. Comfort standards prescribe limits for these parameters.

4.3. RADIANT ASYMMETRY FROM WINDOWS

Many studies emphasize the importance of a warm or a cold window on comfort. By simulating the thermal impacts of ten generic glazing systems ranging from single-pane window to high performance window, Lyons et al. (1999) concluded that except in the case where the body is directly in the sun, long-wave radiation to and from the window is the most significant factor affecting thermal comfort. When applying advanced glazing, a secondary phenomenon occurs.

The inside glass temperature rises. It causes a positive effect in winter, but increases discomfort in summer. Under NFRC summer test conditions, single bronze glazing is 13°C hotter than single clear glazing because of the higher solar absorptance, which corresponds to a calculated increase of discomfort from 36% to 45% due to long-wave radiation. Sengupta et al. (2005) and Chapman et al. (2004) simulated window impacts on comfort for eight cases covering different glass areas and window configurations. By displaying PMV contours on a plane 1.25 m above the floor, the authors showed very large variations due to the existence of the windows.

In summer with solar radiation, the presence of two windows (40% of the wall area) and one window (20% of the wall area) results in only 7% and 25% of the floor area being comfortable (with PMV within -0.5 to $+0.5$). Large glazed façades are essential features of modern architecture. Gan's simulations (2001) showed that when outdoor air temperature is -4°C , room air temperature 21°C , the radiant asymmetry temperature exceeds 10°C when the location is 1 m from the window (room size 5 x 4 x 3 m with a window 3.5 m wide and 2 m high). That means the area within 1 m distance from the window would not meet the ASHRAE standard. Ge and Fazio (2004) measured the inside glass temperatures of a large glass panel when outdoor temperature was -18°C (NFRC winter condition), and Montreal's worst winter condition, -32°C .

The inside glass temperatures were 10°C and 3.8°C , respectively. Improving window performance reduces thermal discomfort. Sengupta et al. (2005) showed that in winter nighttime conditions, changing a single-pane window to double-pane greatly improved the comfortable floor area. Gan (2001) examined a series of factors regarding the window properties, sizes, and shapes. For a single-pane window, a 10°C radiant asymmetry exists at 1 m from window at an outdoor temperature of -4°C .

A double-glazed window has the same asymmetry 0.15 m from the window at an outdoor temperature of -10°C . He also demonstrated that square windows are more likely to cause thermal discomfort than narrow windows and when a large window is replaced by several smaller windows (keeping the same window area), the discomfort is greatly lowered.

Although radiant temperature is as important as air temperature, conventional practice is to use air temperature as the measure for controlling mechanical systems. Gan (2001) recommends that, in circumstances where a large radiant asymmetry exists (e.g. a room with a large window), sensors are more effective if they respond to the combination of air temperature and radiant temperature rather than air temperature alone.

At present the Sun radiates energy at the rate of $(3.9 \times 10^{26} \text{ W})$. At the top of the Earth's atmosphere an average power of (1353 W m^{-2}) is passing through a plane perpendicular to the direction of the Sun. As shown in Fig. 17, regular oscillations around this figure are produced by the changes in the Earth–Sun distance, as the Earth progresses in its elliptical orbit around the Sun.

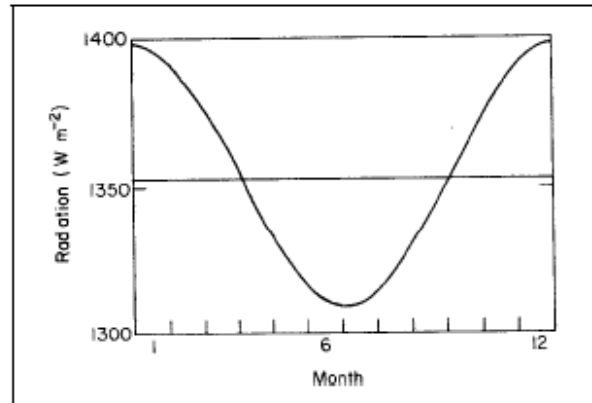


Figure 18 Yearly variations in the “solar constant” (the head-on solar radiation flux at the Earth’s distance; NASA, 1971). The average distance is $(1.5 \times 10^{11} \text{ m})$ and the variation 1.7%. Further variation in the amount of solar radiation received at the top of the atmosphere is caused by slight irregularities in the solar surface, in combination with the Sun’s rotation (about one revolution per month), and by possible time-variations in the surface luminosity of the Sun.

4.4. 3M Window Film

Energy saving films are increasingly being used worldwide to lower building energy costs by reducing excessive solar heat gain through windows. Since the early 1960’s energy saving films have been used as a means to reduce building energy costs. Energy saving window film typically consists of a thin (0.025mm, 0.001 inch) polyester film substrate that has a micro-thin, transparent metal coating applied to one side.



Figure 19 3M window film

This metal coating is applied using vacuum-based technologies such as vapor deposition or sputtering. A second layer of polyester film is laminated over the metal coating to protect the metal. A scratch resistant (SR) coating is applied onto the side of this laminated composite that faces the building interior to protect the film during normal window cleaning. An adhesive layer is applied onto the film side that faces the glass and is protected by a removable release liner until just before the film is applied to the glazing system. UV absorbers are added to the polyester film layers, the adhesive layer, or both to protect from UV degradation. The appearance of film including color, the level of visible light transmission and degree of reflectivity are determined by the metal coating(s) used. Typical all-metal energy films can be silver-reflective, gray, silver-gray, bronze or light green in color. Visible light transmissions (VLT) can vary from very dark (10%) to very light (70%), and the visible reflectance can vary from the same reflectance as clear glass (8%) to highly reflective (60%). The ability of a glazing system to reduce solar heat gain is measured by its solar heat gain coefficient (SHGC). As expected from the variety of films available, the SHGC for window films can vary significantly, from 0.17 to 0.71, as measured on 3mm (1/8 inch) clear glass.

Window film is a retrofit layer applied to the internal or external surface of glass providing a huge range of benefits.

4.4.1) Improving energy efficiency

4.4.2) A comfortable working environment

4.4.3) Safe and more secure

4.4.4) Protection from the sun

4.4.5) Creating privacy

4.4.1. Improving energy efficiency

The use of air conditioning in the UK has rocketed 60% in the past 20 years. But air conditioners are not efficient. Using them to cool a building often uses significantly more energy than it does to heat one.

4.4.2. A comfortable working environment

Studies have shown that variations from 20-23c in workplace temperature have a considerable effect on productivity and quality.

4.4.3. Safe and more secure

Window film helps employers meet their duty of care to staff, adhere to workplace and health and safety regulations and addresses security risks.

4.4.4. Protection from the sun

Sunlight can damage fabrics, furnishings and even skin, but window film can guard against the sun harmful effects.

4.4.5. Creating privacy

Window film can provide privacy in different ways, rendering glazing either one-way, partially or completely opaque.

4.5. Film to glass risk assessment chart

In certain cases, the application of window film can increase the risk of glass breakage or seal failure. The age, condition and type of construction of the glazing system can limit or even prohibit the application of window film. The following film to glass risk. Assessment chart will assist you in determining the risk of glass breakage for specific film to glass type combinations. Ultimately you need to make the final decision with the help of your independent installer.

Table 4 these recommendation are based on solar specifications representing film mounted on 1/8" (3mm) clear glass

FILM TYPE	CLEAR SINGLE PANE	CLEAR DUAL PANE	TINTED SINGLE PANE	TEMPERED TINTED SINGLE PANE	TINTED DUAL PANE
DaylightNatural					
DN 60	L	L	L	L	L
DN 50	L	L	L	L	L
DN 35	L	M	M	L	M
DN 20	M	M	H	M	H
DN 15	H	H	H	M	H
DN 35 EXT	L	L	L	L	L
DN 20 EXT	L	L	M	L	M
Sunset Bronze					
SB 50	L	L	L	L	L
SB 30	L	L	L	L	L
SB 20	L	L	L	L	L
Solar Silver					
SS 35	L	L	L	L	L
SS 20	L	L	L	L	L
SS 35 EXT	L	L	L	L	L
SS 20 EXT	L	L	L	L	L
ScenicView					
SV 40	L	L	L	L	L
SV 30	L	L	L	L	L
SV 10	L	L	L	L	L
NightScape					
NS 35	L	M	M	L	M
NS 25	M	M	H	L	H
NS 15	M	H	H	M	H
NS 05	H	H	H	M	H
Palisade					
PD 55	L	L	L	L	L
PD 45	L	M	M	L	M
PD 35	M	M	H	M	H
Architectural					
MBL 35	L	L	M	L	M
MBL 20	L	L	M	L	M
MGN 35	M	M	H	L	H
MGN 20	M	M	H	L	H
MGD 35	L	L	L	L	L
MGD 20	L	L	L	L	L
Specialty Series					
UV CLEAR	L	L	L	L	L
WHITE FROST	L	L	L	L	L
BLKOUT	H	H	H	H	H

L = Low – Glass breakage or seal failure unlikely

M = Moderate – Window system needs to be carefully inspected and evaluated

H = High – Not recommended due to the high probability of glass breakage or seal failure

5. Solar collectors

Solar energy can be used by three technological processes [Tiwari G.N. et al.(2006)]: chemical, electrical and thermal (Fig.20). Chemical process, through photosynthesis, maintains life on earth by producing food and converting CO₂ to O₂. Electrical process, using photovoltaic converters, provides power for spacecraft and is used in many terrestrial applications. Thermal process can be used to provide much of the thermal energy required for solar water heating and building heating. Another one form of converted solar radiation is mechanical energy as wind and water steams [Weiss, Helsinki et al.(1996)].

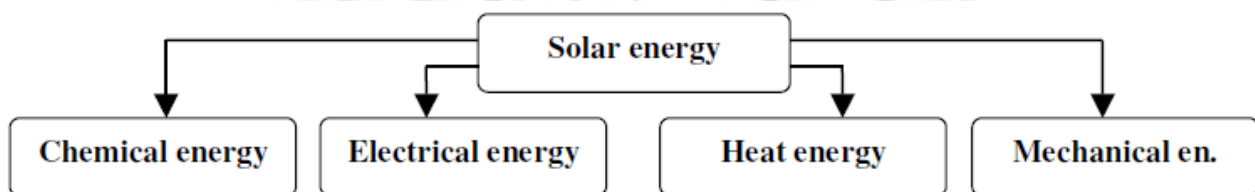


Fig. 20. Conversion of solar radiation to other energy forms

The most important and most expensive single component of an active solar energy system is the collector field, which may be performed in a several versions, as from constructions of solar collectors, as of collector configuration. Solar collector is a mechanical device which captures the radiant solar energy and converts it to useful thermal energy [2007].

The use of solar energy for heat production dates from antiquity. Historically, methods used for collecting and transferring solar heat were passive methods, that is, without active means such as pumps, fans and heat exchangers. Passive solar heating methods utilize natural means such as radiation, natural convection, thermosyphon flow and thermal properties of materials for collection and transfer of heat. Active solar heating methods, on the other hand, use pumps and fans to enhance the rate of fluid flow and heat transfer. Passive systems are defined as systems in which the thermal energy flow is by natural means: by conduction, radiation and natural convection [Yogi goswami et al.(2000)]. Passive features increase the use of solar energy to meet heating and lighting loads and the use of ambient air for cooling. For example, window placement can enhance solar gains to meet winter heating loads, to provide daylighting, or to do both, and this is passive solar use.

A distinction is made between energy conservation techniques and passive solar measures. Energy conservation features are designed to reduce the heating and cooling

energy required to thermally condition a building. Such features would include the use of insulation to reduce heating or cooling loads. Similarly, window shading or appropriate window placement could lower solar gains, thus reducing summer cooling loads. An example of active solar system is solar collector and thermo battery and of passive solar system – south side windows and greenhouse.

Converting the sun's radiant energy to heat is the most common and well-developed solar conversion technology today. The temperature level and amount of this converted energy are the key parameters that must be known to match a conversion scheme to a specific task effectively. Possible achievable temperature depending of concentration level in Table 5 is shown.

Table 5 Classification of solar collectors according to concentration degree

Category	Example	Temperature range, °C	Efficiency, %
No concentration	Flat-plate Evacuated tube	up to 75 up to 200	30 – 50
Medium concentration	Parabolic cylinder	150 - 500	50 – 70
High concentration	Parabodial	1500 and more	60 - 75

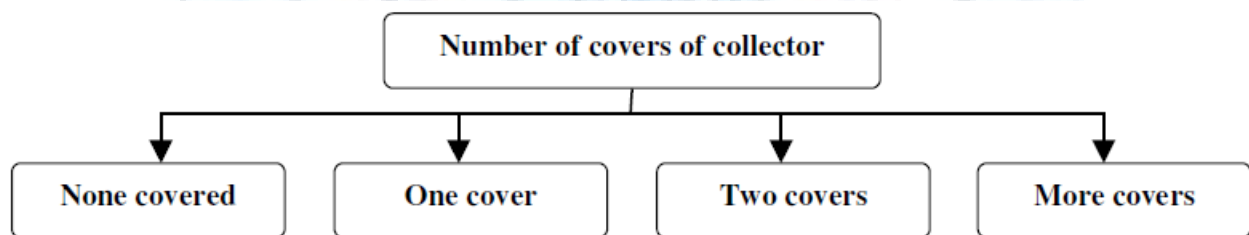


Fig. 21. Number of covers of solar collector

In way of enlarge of number of covers heat losses become reduced, but it must be taken into account that solar income are reduced too. For a system of N covers all of the same materials, a following analysis yields. Equation for estimation of transmittance for both parallel and perpendicular components of polarization r_N for a several number of cover N by following equation is given [Duffie.J.A,Beckman et al.(2006)]:

$$\tau_{rN} = \frac{1}{2} \left[\frac{1-r_{II}}{1+(2N-1)r_{II}} + \frac{1-r_{\perp}}{1+(2N-1)r_{\perp}} \right] \quad (1)$$

Where r_{II} – parallel component of unpolarized radiation, non dimensional value;
 r_{\perp} - Perpendicular component of unpolarized radiation, non dimensional value;
 N – number of covers.

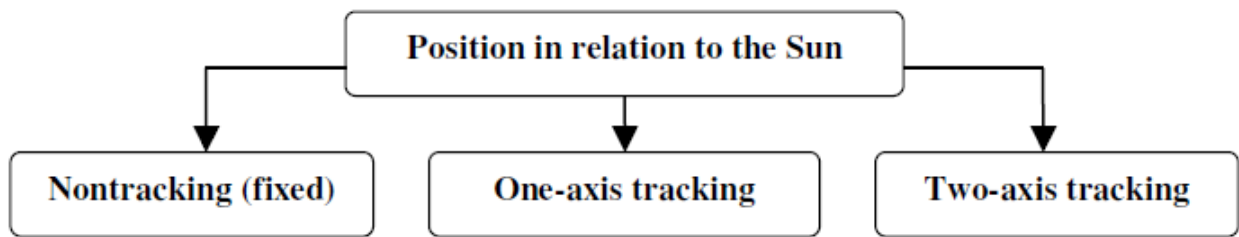


Fig. 22. Equipment ratio of the collector

It is well known that the maximum gain from solar collector it is possible to obtain when solar rays are striking solar device perpendicularly because of reflective losses from device surface. In that case solar collectors are divided in three designs shown in Fig.22. Must be mentioned, that the equipment of collector with tracking devices increase its costs. Consider accordant literature where gathered information about five mine types of solar collectors described below.

5.1. Types of solar collectors

5.1.1. Tank-type collector

In an Integral Collector Storage unit, the hot water storage tank is the solar absorber. The tank or tanks are mounted in an insulation box with glazing on one side and are painted black or coated with a selective surface.

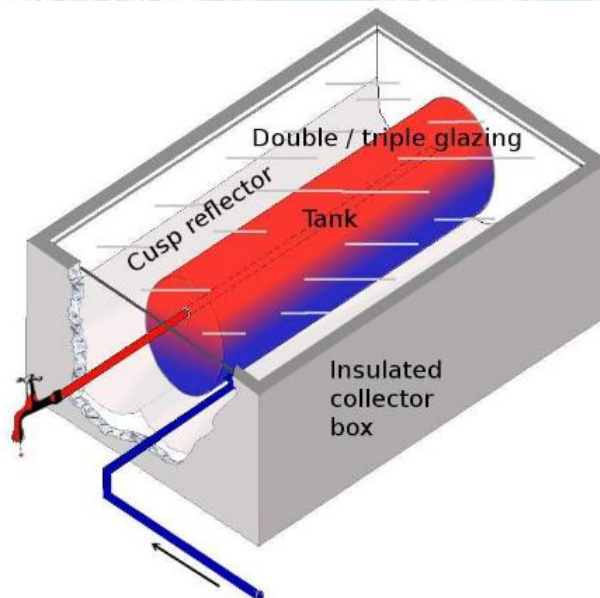


Figure 23 tank type collector

The sun shines through the glazing and hits the black tank, warming the water inside the tank. The single tanks are typically made of steel, while the tubes are typically made of copper [Ramlow B., Nusz B et al.(2007)].

Achievable temperature with such collectors is a little bit less than in flat-plate collectors (see Table 5).

5.1.2. Pool collector

The single largest application of active solar heating systems is in heating swimming pools. Special collectors have been developed for heating seasonal swimming pools: they are unglazed and made of a special copolymer plastic. These collectors cannot withstand freezing conditions. Approximate maximum operating temperature of such type of solar collector is 10 – 20 °C [Rabi.A et al.(1985)] above ambience.

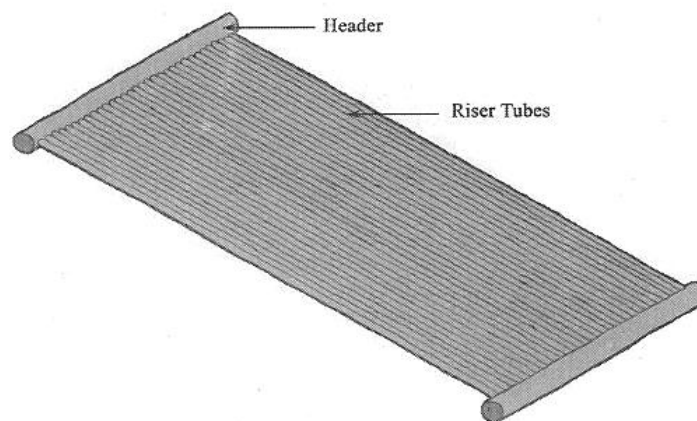
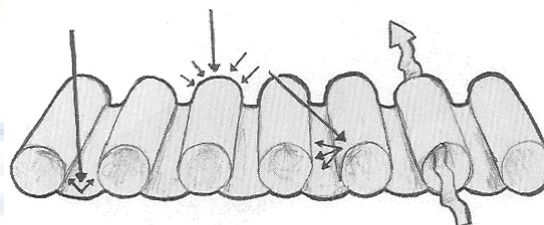


Figure 24 sketch of a pool collector



Web and tube configuration

Figure 25 sketch of the tubes of a pool collector

5.1.3. Flat-plate collector

Flat-plate collectors are the most widely used kind of collectors in the world for domestic solar water heating and solar space heating applications. Flat-plate collectors are used typically for temperature requirements up to 75 °C (Table 5) although higher temperatures can be obtained from high efficiency collectors (there water must be changed to other heat transfer liquid because of its boiling temperature of 100 °C).

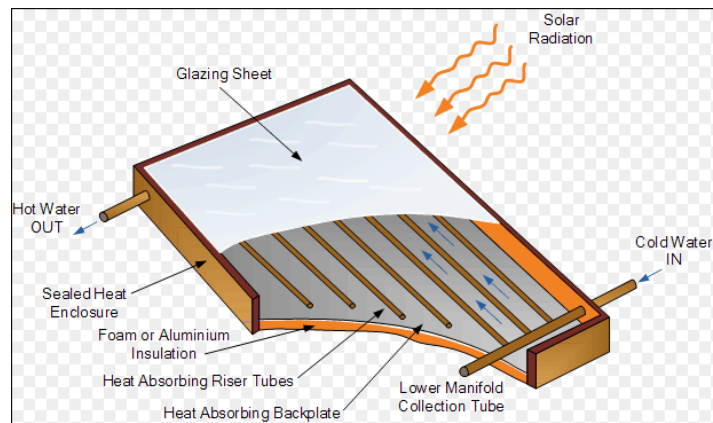


Figure 26 Flat plate collector

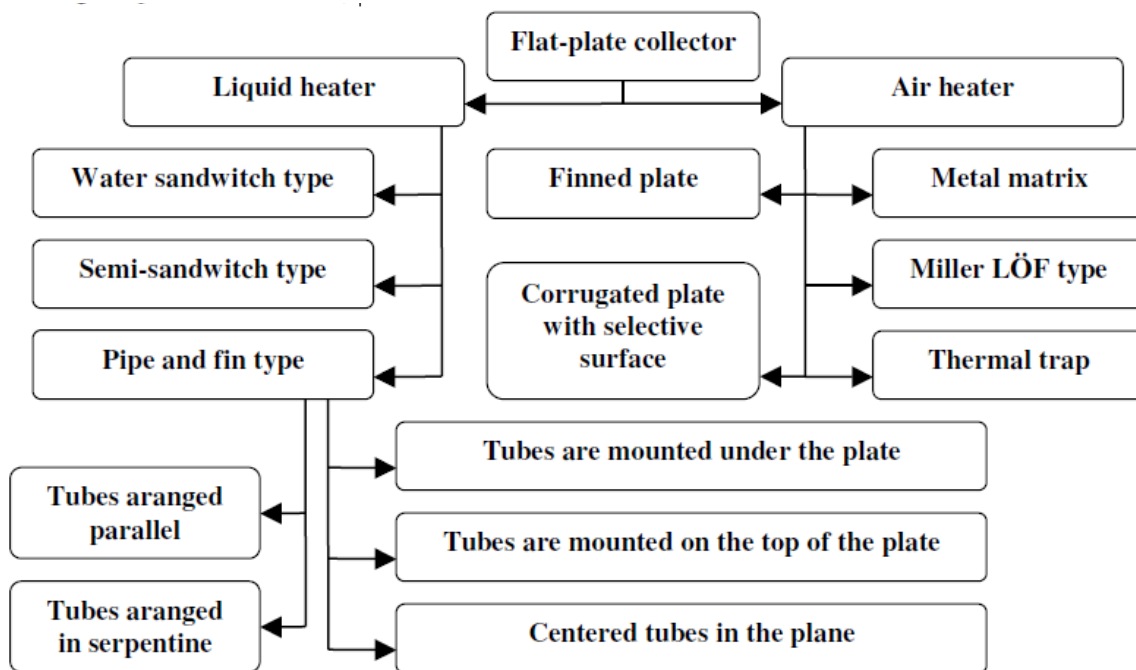


Fig. 27. Classification of flat-plate solar collectors

These collectors are of two basic types based on heat transfer fluid [Yogi goswami et al.(2000)]: liquid type and air type (Table 6). Flat-plate collectors use both beam and diffuse solar radiation, do not require tracking of the sun, and require little maintenance [Duffie.J.A,Beckman et al.(2006)], is usually planed on the top of a building or other structures.

Flat-plate collectors are durable and effective. These collectors have a distinct advantage over other types in that they shed snow very well when installed in climates that experience significant snowfall. They are the standard to which all other kinds of collectors are compared. Depending on absorbers' construction and configuration flat-plate collectors are divided in several types (Fig. 27).

Table 6 Classification of collectors according to heat transfer medium

Heating matter	Efficiency, %	Achievable temperature, °C
Liquid heaters	30 - 75	75 – 1500 and more
Air heaters	30 – 65	30 – 80

Because of their high heat loss coefficient, ordinary flat-plate collectors are not practical for elevated temperatures, say above 80 °C. When higher temperatures are desired, one needs to reduce the heat loss coefficient. This can be accomplished principally by two methods: evacuation and concentration, either singly or in combination. While several attempts have been made to build evacuated flat plates, they do not seem to hold any promise of commercial success.

5.1.4. Evacuated tube collector

While flat-plate collectors are all essentially made the same way and perform the way from one brand to other, evacuated tube collectors vary widely in their construction and operation. Evacuated tube collectors are constructed of a number of glass tubes. Each tube is made of annealed glass and has an absorber plate within the tube, because tube is the natural configuration of an evacuated collector [Rabi.A et al.(1985)].

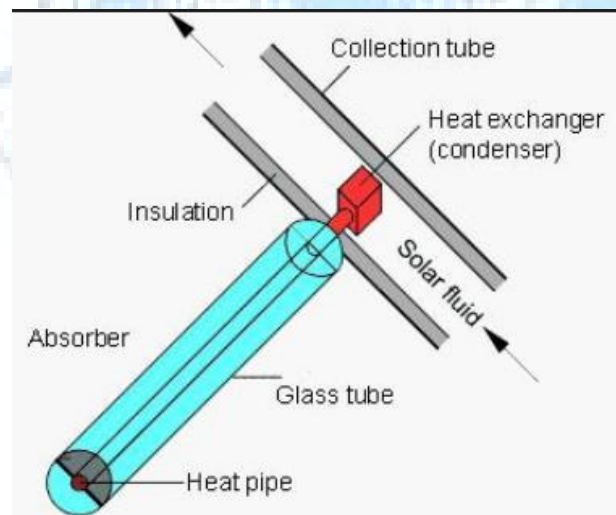


Figure 28 Evacuated tube collectors

During the manufacturing process in order to reduce heat losses through conduction and convection, a vacuum is created inside the glass tube. The only heat loss mechanism remaining is radiation [Tiwari G.N et al. (2006)]. The absence of air in the tube creates excellent insulation, allowing higher temperatures to be achieved at the absorber plate. In order to improve an efficiency of evacuated tube collector there are several types of concentra-

tors depending on its concave radius established. Classification of evacuated solar collectors in Fig. 29 is shown.

There are many possible designs of evacuated collectors, but in all of them selective coating as an absorber is used because with a nonselective absorber, radiation losses would dominate at high temperatures, and eliminating convection alone would not be very effective [Rabi.A et al.(1985)].

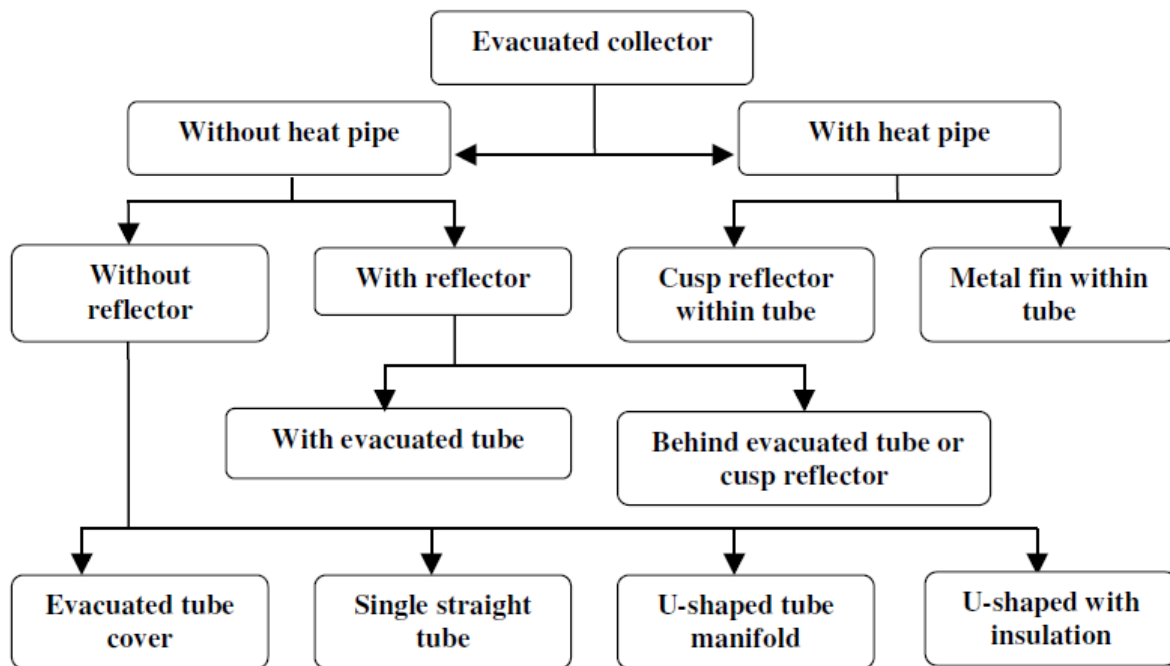


Fig. 29. Classification of evacuated solar collector

A heat pipe provides the most elegant way of extracting heat from an evacuated collector. Heat pipe is hermetically sealed tube that contains a small amount of heat transfer liquid. When one portion of tube is heated the liquid evaporates and condenses at the cold portion, transferring heat with great effectiveness because of the latent heat of condensation. The heat pipe contains a wick or is tilted (or both) to ensure that the liquid follows back to the heated portion to repeat the cycle. It is easy to design a heat pipe (e.g., by giving it the proper tilt) so that it functions only in one direction.

This thermal diode effect is very useful for the design of solar collectors, because it automatically shuts the collector off and prevents heat loss when there is insufficient solar radiation. Also, heat pipes have lower heat capacity than ordinary liquid-filled absorber tubes, thus minimizing warm-up and cool down losses [Rabi.A et al.(1985)].

Heat pipe provides the method of transferring larger amounts of heat from the focal area of a high-concentration solar collector to a fluid with only small temperature difference. It consists of a circular pipe with an annular wick layer situated adjacent to the pipe wall. The circular pipe is perfectly insulated from outside to avoid thermal losses from the circular

pipe. Solar energy falls on evaporator and the fluid inside evaporator boils. The vapor migrates to the condenser where heat of vapor is transferred to a circulation fluid loop. The heat available with circulating fluid is further carried away to the end use point. The circulation fluid after releasing its heat is transferred to the boiler by capillary action in the wick or by gravity and cycle repeats. Gravity return heat pipes can operate without wick but cannot be operated horizontally as a result.

5.1.5. Concentrating collector

A concentrating collector utilizes a reflective parabolic-shaped surface to reflect and concentrate the sun's energy to a focal point or focal line where the absorber is located. To work effectively, the reflectors must track the sun.

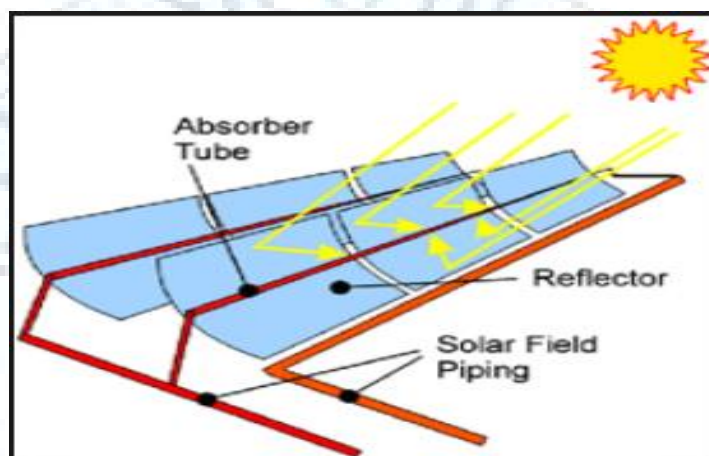


Figure 30 concentrating collector

These collectors can achieve very high temperatures (Table 5) because the diffuse solar resource is concentrated in a small area. The area geometrical concentration ratio according to [Tiwari G.N. et al.(2006)] is

$$C = \frac{A_a}{A_r} = \frac{R^2}{r^2} = \frac{1}{\sin^2 \theta_s} \quad (2)$$

where C – concentration ratio, non-dimensional value;

A_a – area of the collecting aperture, m^2 ;

A_r – area of the absorber, m^2 ;

R – distance from the sun to the concentrator, m;

r – radius of the sun, m;

θ_s – half of an angle subtended by the sun, °.

This ratio has an upper limit that depends on whether the concentration is a three-dimensional (circular) concentrator such as a paraboloid or two-dimensional (linear) concentrator such as a cylindrical parabolic concentrator. Thus, the maximum possible con-

centration ratio in air for circular concentrators is 45, and for linear concentrators the maximum is 212 [Duffie J.A, Beckman et al. (2006)].

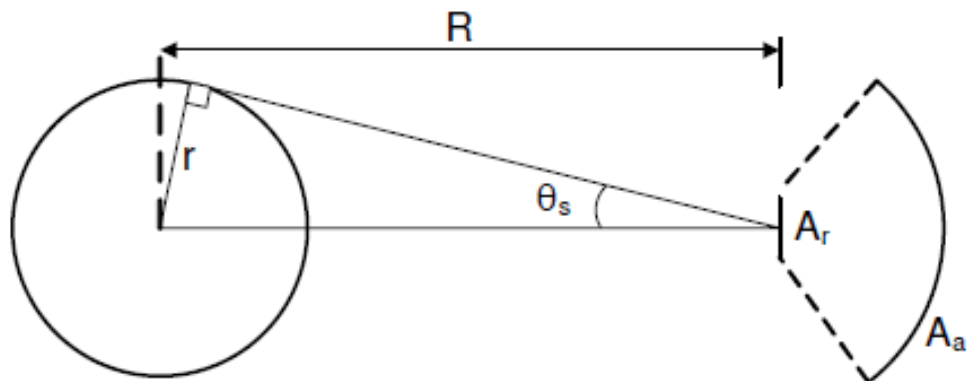


Fig. 31. Schematic of the sun at a distance R from a concentrator [2, 5, 6]:

R = distance from the sun to the concentrator, m ;

r = radius of the sun, m ;

s = half of an angle subtended by the sun, $^\circ$;

A_r = area of the absorber, m^2 ;

A_a = area of the collecting aperture, m^2

Solar concentrator may be classified as tracking type and non-tracking type. Tracking may be continuous or intermittent and may be by one-axis or two-axis (Fig. 31). As the sun may be followed by moving either the focusing part or the receiver or both; concentrators can be classified accordingly. Further, the system may have distributed receiver or central receiver. The concentrators may also be classified on the basis of optical components. They may be reflecting or refracting type, imaging or non-imaging type, and line focusing or point focusing type. The reflecting or refracting surface may be one piece or a composite surface; it may be a single or two stage type systems and may be symmetric or asymmetric. In practice, however, hybrid and multistage systems, incorporating various levels of the features, occur frequently. Types of concentrators in Fig.32 are shown.

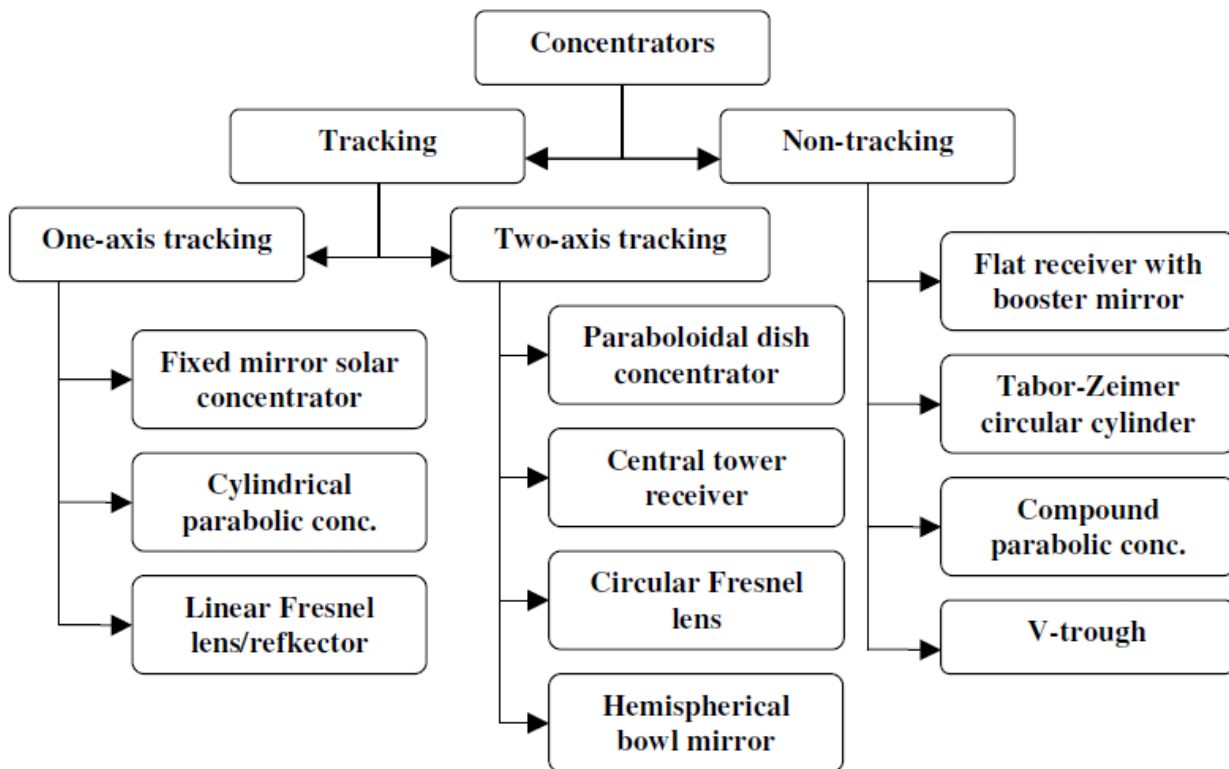


Fig. 32. Classification of concentrators

6. HEAT BALANCE

6.1 Energy balance of the collector.

In order to define the energy balance of the solar air collector the following equation shall be used:

$$Q_u = A_c F_R [S - U_L (T_{fm} - T_a)] \quad [W] \quad (3)$$

Where:

A_c = collector area [m^2],

F_R = heat removal factor,

S = absorbed solar radiation per unit area [$\frac{W}{m^2}$],

U_L = collector overall heat loss coefficient [$\frac{W}{m^2.K}$],

T_{fm} = mean fluid temperature [K],

T_a = ambient temperature [K].

6.2. Heat removal factor

Heat removal factor – relates the actual useful energy gain of a collector to the useful gain if the whole collector surface were at the fluid inlet temperature.

In order to calculate the heat removal factor some partial equations need to be solved.

Radiation heat transfer coefficient:

$$h_r = \frac{4 \cdot \sigma \cdot T_{fm}^3}{\frac{1}{\varepsilon_1} + \frac{1}{\varepsilon_2} - 1} \quad \left[\frac{W}{m^2 \cdot K} \right] \quad (4)$$

σ = Stefan – Boltzmann constant $\left[\frac{W}{m^2 \cdot K^4} \right]$,

T_{fm} = mean fluid temperature [K],

ε_1 = emittance of glass,

ε_2 = emittance of plate,

Reynolds number:

$$Re = \frac{\dot{m} D_h}{A_f \mu} \quad (5)$$

\dot{m} = flow rate [kg/s],

D_h = hydraulic diameter; for flat plates is twice the plate spacing [m],

A_f = fluid area (air channel depth times width) [m²],

μ = dynamic viscosity [kg/(s·m)].

Nusselt number

$$Nu = 0,0158 * Re^{0,8} \quad (6)$$

Heat transfer coefficient

$$h = Nu \cdot \frac{k}{D_h} \quad \left[\frac{W}{m^2 \cdot K} \right] \quad (7)$$

k = thermal conductivity [W/m·K].

Heat removal factor:

$$F' = \left[1 + \frac{U_L}{h + \left(\frac{1}{h} + \frac{1}{h_r} \right)^{-1}} \right]^{-1} \quad (8)$$

$$F'' = \left[\dot{m} C_p / (A_c U_L F') \right] \left[1 - \exp \left(- \frac{A_c U_L F'}{\dot{m} C_p} \right) \right] \quad (9)$$

$$F_R = F' \cdot F'' \quad (10)$$

Where:

\dot{m} = flow rate [kg/s],

C_p = specific heat [kJ/kg·K]

6.3. Absorbed solar radiation

$$S = I_b R_b (\tau\alpha)_b + I_d (\tau\alpha)_d \left(\frac{1+\cos\beta}{2} \right) + \rho_g (I_b + I_d) (\tau\alpha)_g \left(\frac{1-\cos\beta}{2} \right) \quad \left[\frac{W}{m^2} \right] \quad (11)$$

Absorbed solar radiation consists of three different radiations. Index b means beam radiation (direct), index d – diffuse radiation, index g – ground-reflected radiation.

I = irradiation $\left[\frac{W}{m^2} \right]$,

R_b = ratio of beam radiation on the tilted surface to that on horizontal surface,

τ = transmittance,

α = absorptance,

$(1 + \cos\beta)/2$ and $(1 - \cos\beta)/2$ – view factors from the collector to the sky and from the collector to the ground respectively,

ρ_g = ground reflectance,

For a vertical collector the above equation is transformed into:

$$S = I_b R_b (\tau\alpha)_b + \frac{1}{2} I_d (\tau\alpha)_d + \frac{1}{2} \rho_g (I_b + I_d) (\tau\alpha)_g \quad \left[\frac{W}{m^2} \right] \quad (12)$$

7. Heat losses

7.1. Window

The heat losses through the window will be due to both conduction and convection.

$$A_{window} = 34.02 \times 3.4 = 115.67 \text{ m}^2$$

Conduction For the entire window,

$$Q_{cond} = U_{window} * A_{window} * (T_{int} - T_{ext}) = 5.7 * 115.67 * (T_{int} - T_{ext}) \quad (13)$$

where,

Q_{cond} = is the heat flux, [W]

the window surface [m²]

T_{int} = is the internal ambient temperature, [°C]

T_{ext} = is the external ambient temperature, [°C]

U_{window} = is the U-value for the window, $\left[\frac{W}{m^2 \cdot K} \right]$

Convection (plumes)

Plumes are produced by convection as a result of difference in temperature (buoyancy) between the air in contact with the cold surface of the window. In this way, buoyant forces are generated which cause this layer of air adjacent to the window to flow in a downward direction. This layer of air adjacent to the wall, to which vertical motion is confined, is

called the natural convection boundary layer. The boundary layer begins with zero thickness at the top of the vertical wall and increases in thickness in the downward direction [Heiselberg et al., (1994)].



Figure 33. Plume for a cold surface

The flow of air for the laminar and turbulent layers for a vertical surface can be calculated according to the following equations [Manz, H and Frank, T (2004)].

$$\text{Laminar boundary layer : } q = 2.87 * 10.3L (T_{surf} - T_{int})^{\frac{1}{4}} H^{\frac{3}{4}}$$

$$\text{Turbulent boundary layer : } q = 2.75 * 10.3L (T_{surf} - T_{int})^{\frac{2}{5}} H^{\frac{6}{5}}$$

Where,

q = is the volume flow rate [m^3/s]

L = is the length of surface [m]

H = is the height of surface [m]

T_{surf} and T_{int} are the surface and air temperatures ($^{\circ}\text{C}$)

For this case, the flow to be considered is just laminar because of very low flow movements take place there. If it supposed that T_{surf} is approximately T_{ext} for one pane windows,

$$q = 2.87 * 10.3L(T_{ext} - T_{surf})^{\frac{1}{4}} H^{\frac{3}{4}} = 2.87 * 10.3 * 3.4 * (T_{int} - T_{ext})^{\frac{1}{4}} 34.02^{\frac{3}{4}} \quad (14)$$

According to this, the heat transfer due to convection can be calculated as follows,

$$Q_{conv} = \dot{q} \rho C_p (T_{int} - T_{ext}) \quad (15)$$

The basic factors determining air speed close to the window are the height of the cold surface and the temperature difference between the surface and the air in the room.

7.2. Collector overall heat loss coefficient

$$U_L = U_t + U_b + U_e \quad \left[\frac{W}{m^2 \cdot K} \right] \quad (16)$$

Where:

U_t = top loss coefficient $\left[\frac{W}{m^2 \cdot K} \right]$,

U_b = the energy loss through the bottom of the collector $\left[\frac{W}{m^2 \cdot K} \right]$,

U_e = edge losses $\left[\frac{W}{m^2 \cdot K} \right]$.

7.2.1. Top loss coefficient

$$U_t = \left\{ \frac{N}{\frac{c}{T_{pm}} \left[\frac{(T_{pm} - T_a)}{(N+f)} \right]^e} + \frac{1}{h_w} \right\}^{-1} + \frac{\sigma (T_{pm} + T_a) (T_{pm}^2 + T_a^2)}{(\varepsilon_p + 0,00591 N h_w)^{-1} + \frac{2N+f-1+0,133\varepsilon_p}{\varepsilon_g} - N} \quad (17)$$

U_t = top loss coefficient $\left[\frac{W}{m^2 \cdot K} \right]$,

N = number of glass covers,

$f = (1 + 0,089h_w - 0,1166h_w\varepsilon_p)(1 + 0,07866N)$,

$C = 520(1 - 0,000051\beta_2)$ for $0^\circ < \beta < 70^\circ$

For $70^\circ < \beta < 90^\circ$ use $\beta = 70^\circ$,

$e = 0,430(1 - 100/T_{pm})$,

β = collector tilt (degrees),

ε_g = emittance of glass,

ε_p = emittance of plate,

T_a = ambient temperature [K],

T_{pm} = mean plate temperature [K],

h_w = wind heat transfer coefficient $\left[\frac{W}{m^2 \cdot K} \right]$,

σ – Stefan – Boltzmann constant $\left[\frac{W}{m^2 \cdot K^4} \right]$.

Wind heat transfer coefficient:

$$h_w = \frac{8,6 \cdot V^{0,6}}{L^{0,4}} \quad \left[\frac{W}{m^2 \cdot K} \right] \quad (18)$$

Where:

V = wind speed $\left[\frac{m}{s} \right]$

L = cube root of the house volume [m]

7.2.2. Energy loss through the bottom of the collector

$$U_b = \frac{K}{L} \quad \left[\frac{W}{m^2 \cdot K} \right] \quad (19)$$

K = insulation thermal conductivity $\left[\frac{W}{m \cdot K} \right]$,

L = thickness of insulation $[m]$.

7.2.3. Edge losses

$$U_e = \frac{(UA)_{\text{edge}}}{A_c} \quad \left[\frac{W}{m^2 \cdot K} \right] \quad (20)$$

$(UA)_{\text{edge}}$ = edge loss coefficient-area product

7.2.4. DUCT AND PIPE LOSS FACTORS

The energy lost from ducts and pipes leading to and returning from the collector in a solar energy system can be significant. Beckman (1978) has shown that the combination of pipes or ducts plus the solar collector is equivalent in thermal performance to a solar collector with different values of U_L and $(\tau\alpha)$. (For simplicity in terminology, the term duct will be used, but the same analysis holds for pipes. Losses from ducts are more likely to be a problem than those from pipes.)

Consider the fluid temperature distribution shown in Figure 34. Fluid enters the portion of the duct from which losses occur 2 at temperature T_i . Due to heat losses to the ambient at temperature T_a , the fluid is reduced in temperature by an amount ΔT_i before it enters the solar collector. The fluid passes through the collector and is heated to the collector outlet temperature. This temperature is then reduced to T_o as the fluid loses heat to the ambient while passing through the outlet ducts. From energy balance considerations the useful energy gain of this collector-duct combination is equal to

$$Q_u = (\dot{m} C_p)_c (T_o - T_i) \quad (21)$$

This energy gain can also be related to the energy gain of the collector minus the duct losses by the following rate equation:

$$Q_u = A_c F_R [G_T (\tau\alpha) - U_L (T_i - \Delta T_i - T_a)] - \text{losses} \quad (22)$$

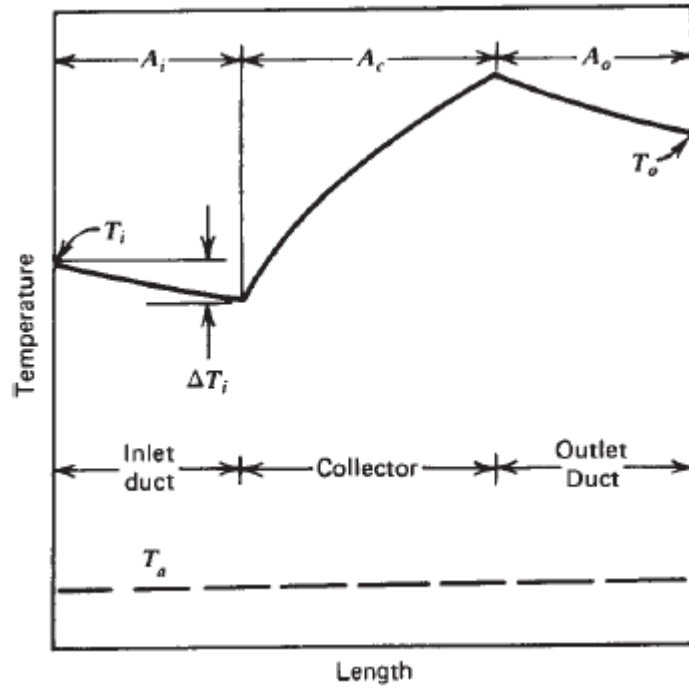


Figure 34 fluid temperature distribution

The duct losses are equal to the integrated losses over the inlet and outlet ducts and are given by

$$\text{Losses} = U_d \int (T - T_a) da \quad (23)$$

Where U_d is the loss coefficient from the duct. It is possible to integrate but in any well-designed system the losses from ducts must be small and the integral can be approximated to an adequate degree of accuracy in terms of the inlet and outlet temperatures:

$$\text{Losses} = U_d A_i (T_i - T_a) + U_d A_o (T_o - T_a) \quad (24)$$

where A_i and A_o are the areas for heat loss of the inlet and outlet ducts. Upon rearranging Equations (21) and (24), the losses can be expressed in terms of the useful energy gain and the inlet fluid temperature as

$$\text{Losses} = U_d (A_i + A_o) (T_i - T_a) + \frac{U_d A_o Q_u}{(\dot{m} C_p)_c} \quad (25)$$

The decrease in temperature, T_i , due to heat losses on the inlet side of the collector can be approximated by

$$T_i = [U_d A_i (T_i - T_a)] / (\dot{m} C_p)_c \quad (26)$$

Substituting Equations (25) and (26) into (22) and rearranging, the useful energy gain of the collector and duct system can be expressed as

$$Q_u = \frac{A_c F_R \left[G_T(\tau\alpha) - U_L \left(1 - \frac{U_d A_i}{(\dot{m} C_p)_c} + \frac{U_d (A_i + A_o)}{A_c F_R U_L} \right) (T_i - T_a) \right]}{1 + \frac{U_d A_o}{(\dot{m} C_p)_c}} \quad (27)$$

Equation (27) can be made to look like the usual collector equation by defining modifies values of $(\tau\alpha)$ and U_L so that

$$Q_u = A_c F_R [G_T(\tau\alpha)' - U'_L (T_i - T_a)] \quad (28)$$

Where

$$\frac{(\tau\alpha)'}{(\tau\alpha)} = \frac{1}{1 + \frac{U_d A_o}{(\dot{m} C_p)_c}} \quad (29)$$

And

$$\frac{U'_L}{U_L} = \frac{1 - \frac{U_d A_i}{(\dot{m} C_p)_c} + \frac{U_d (A_i + A_o)}{A_c F_R U_L}}{1 + \frac{U_d A_o}{(\dot{m} C_p)_c}} \quad (30)$$

8. Heat losses reduce

There are different optimization approaches to reduce the heat loss from windows. Both the glazing and frame can be made some change in order to reduce the convection or conduction heat transfer. This section will gradually introduce some technology or reasonable method and outcome problem then explain in detail.

8.1. Optimization of glazing

Current main technology based on the multi-layer glazing window, vacuum glazing system, gas filling window, and low-emittance coating cavity.

8.1.1. Multi-layer glazing windows

In Sweden, the window of modern buildings and not too old houses are constructed as two glazing window, but for some developing country, such as China, large amounts 11 of building window or single house window are still the one glazing window. The different between this two is the inside gap contains or not, it could be filling with air and other gas, or just vacuum. A case study is done by Korea scientists (Songa, et al, 2007) about the U-value of different glazing layer, it shows an obvious changes. It can be

seen from Table 7 that with the increase of glazing layer, the U-value is decrease. It has nothing to do with what kind of frame it would be, and it has no related to what kind of assignments is done within the gap of layers.

Table 7, U-value of different glazing layer (table source: Songa, et al, 2007)

Type of glazing	Required overall heat transfer coefficient (U , $W/m^2 \text{ } ^\circ C$) according to the material of window frame and the minimum temperature difference ratio to satisfy the insulation performance requirement (T_{DRW})								
		Metal				Wood		Plastic	
		Without thermal breaker		With thermal breaker		6	12	6	12
		6	12	6	12				
Gas layer thickness (mm)									
Double glazing	U	4.19	3.80	3.60	3.30	3.30	3.00	3.30	3.00
	T_{DRW}	0.49	0.64	0.57	0.60	0.60	0.64	0.60	0.64
Double glazing (Low-e)	U	3.70	3.20	3.10	2.60	2.90	2.40	2.90	2.40
	T_{DRW}	0.55	0.61	0.63	0.69	0.65	0.71	0.65	0.71
Double glazing (Argon-filled)	U	4.00	3.70	3.37	3.20	3.10	2.90	3.10	2.90
	T_{DRW}	0.52	0.55	0.59	0.61	0.63	0.65	0.63	0.65
Double glazing (Low-e, argon-filled)	U	3.37	2.90	2.80	2.40	2.60	2.20	2.60	2.20
	T_{DRW}	0.59	0.65	0.66	0.71	0.69	0.73	0.69	0.73
Triple glazing	U	3.37	3.20	2.90	2.60	2.60	2.40	2.60	2.40
	T_{DRW}	0.59	0.61	0.65	0.69	0.69	0.71	0.69	0.71
Single glazing	U	6.60		6.10		5.30		5.30	
	T_{DRW}	0.20		0.26		0.36		0.36	

According to the common sense, by increasing more and more glazing, the window must be getting a good insulation property. But beyond the limitation, the weight and installation problem is coming.

8.1.2. Vacuum glazing

For double or triple glazing window, the air in the gap between each glass sheets can be extracting out to form a vacuum space. Therefore the heat transfer will minimize because of the gaseous heat transfer is negligible, and the internal vacuum space can be stable for a long period in terms of current technology. There are apparently potential benefits of vacuum glazing. Firstly, by combination of a vacuum space and low emittance coating, a very high level of thermal insulation could be achieved. Secondly, since the insulating properties of an evacuated space are effectively independent of the width of the space, a narrow vacuum space could be constructed which get good thermal insulation and saves the whole windows volume at the same time (Collins & Simko, 1998). It still meets the challenges in design and manufacture.

A good thermal insulation cannot be achieved if the atmospheric pressure is higher than 10^{-6} pa; therefore it is essential to maintain an absolutely hermetic space with a sealed edge.

Hermetic condition needs the temperature of around 500°C to achieve during the manufacture, the low emittance coating which used to decrease radiative heat flow between the glass sheets must be survive without degradation.

The whole glazing is under the effect of atmospheric pressure. A glass cylinder can hold almost 100 kpa pressure different associated with internal vacuum, but it is easier to fracture for a plate glazing pane. Under this circumstance, the support pillars are considerable to build within the gap to overcome the high pressure effect. Simultaneously, the pillars are a kind of thermal bridge, it forms an approach to contact indoor and outdoor climate, which is a short cut to waste energy. There is an unbalance between support components and the vacuum space. On the other hand, the support pillars must be sufficiently small to meet the demand.

In this vacuum design, the temperature differentials result in significant 13 mechanical tensile stresses. The structure must be able to withstand the differential thermal expansion of two glass sheets. So far, there are two strategies to deal with this problem. One is use a flexible metal edge seal that permits the lateral movement between glass sheets, therefore the glass sheets will slide over the support pillars and it must built a glass-to-metal seal edge; another is that the edge of two glass sheets must be rigid fused, and requires a glass-to-glass seal, it also should permits a little bit lateral movement. Now days there still tricky to make a flexible edge for vacuum glazing (Collins & Simko, 1998).

8.1.3. Basic Fabrication

A sample of Collins & Simko work can be seen from Figure 35. The vacuum glazing is made by thickness of 3 mm or 4 mm soda-lime glass with low emittance surface of inner face; The pillars are made from a high strength, heat resistant, nickel-based alloy named Inconel 718. They are typically 0.25 mm in diameter and 0.15 mm in height. Based on their research of relation between the diameter and length of pillars, typically, vacuum glazing is designed with a glass-to-glass pillar conductance of between 0.40 W/m²K (for 4 mm thick glass, with $p=25$ mm and $a=0.125$ mm), and 1.2 w/m²k (for 3 mm thick glass with $p=20$ mm and $a=0.25$ mm)

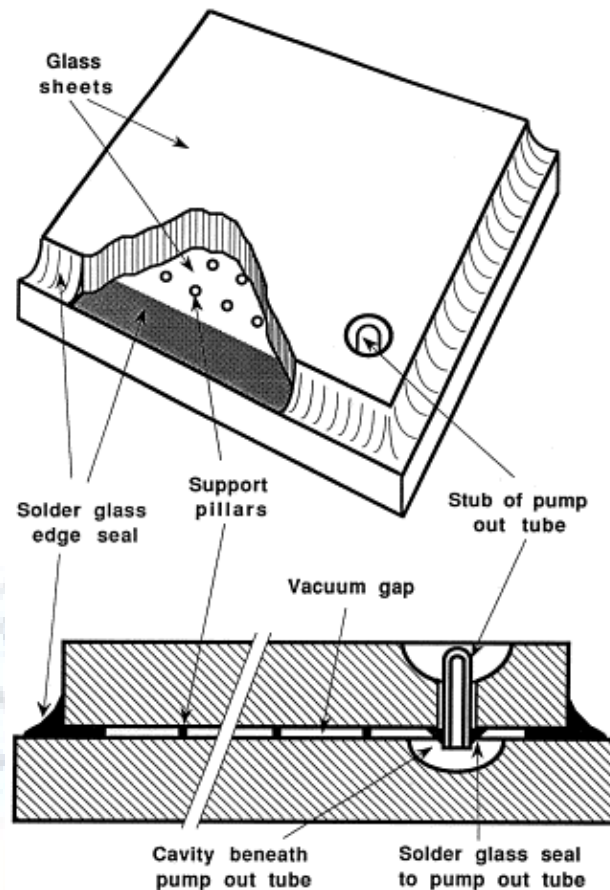


Figure 35, Schematic of vacuum glazing, as produced at the University of Sydney. (figure source: Collins & Simko, 1998)

8.1.4. Gas filled glazing

This kind of optimization is filling gas with good thermal property between each 17 glazing and gets a reduction of heat loss. The most common material is absorbing gas, the rest are silica aerogel, chromogenic materials and phase change materials (PCM) (Ismail, et al. 2007). Usually, the gas filled window can be fill with lots kind of gas, these gas sometime are noble gas or some simple gas such as the carbon dioxide (see Figure 36). For safety and valid, the filled gas must be non-toxic, low conductivity and get high viscosity.

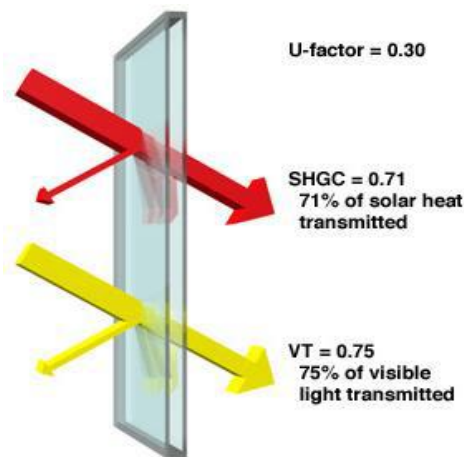


Figure 36, the gas filled window sample

The window in Figure 36 is done by University of Minnesota, the noble gas argon is filled in the window. This kind of window be designed to reduce heat loss while admit the solar gain, it has low emissivity glass which can reduce heat loss in winter and refuse outdoor heat come inside in summer. In terms of the project, the U-value is achieved around 0.3 W/m²K (Arasteh. et al).

Another great research is to fill in glazing cavity with SF₆, CO₂, NO₂ and NH₃ or some other gases. The range of the width between each glazing was set from 6 to 20 mm, and kept at a steady state; uncoated clear-silica glass has a hemispherical surface emittance of 0.84. In coated-glass case, the surface of the glass which expose to indoor was assume to have an emittance of 0.065; the convergence criteria requires that the heating energy flux leaving the exterior surfaces agree to within 0.5 W/m²K with each other, and the residual from each energy balance be less than 0.2 W/m²K 18 (Reilly, et al.1990). The heat transfer process includes energy conducts, transmits, absorbs and emits thermal radiation. During the modeling, their result in Figure 37 and Figure 38 shows the relation between the gap width and the U-value

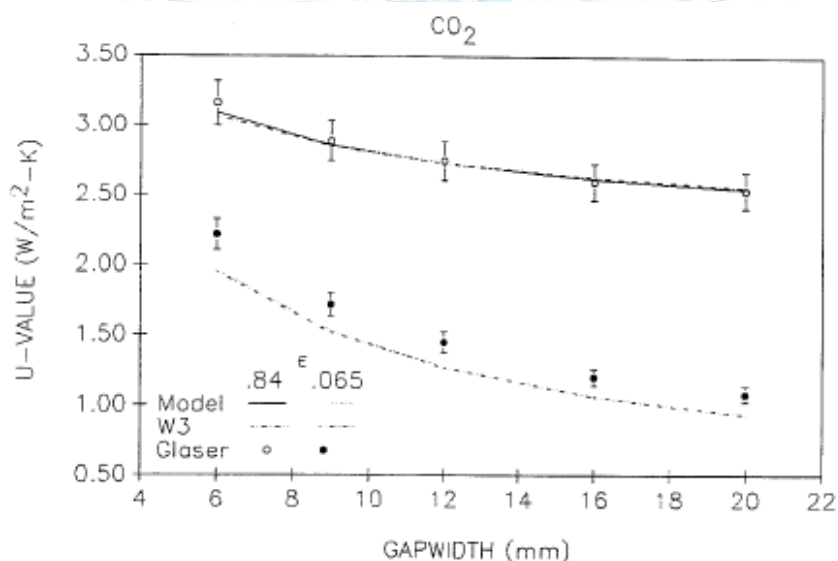


Figure 37, The relation between gap width and the U-value of CO₂ as media

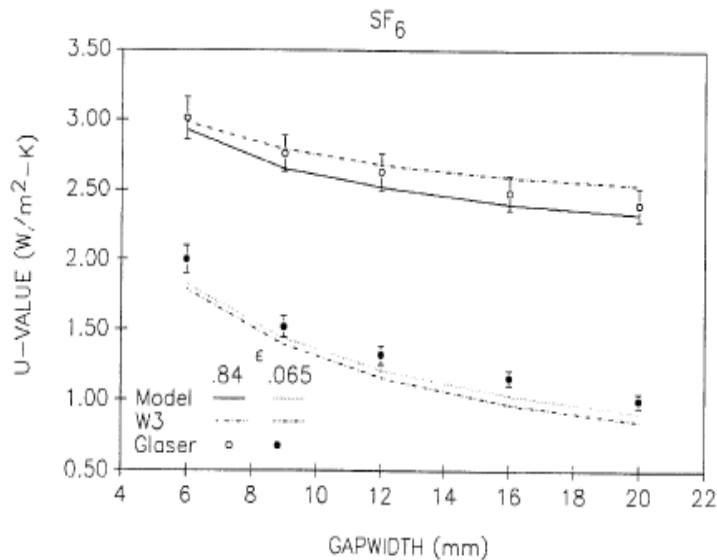


Figure 38, The relation between gap width and the U-value of SF6 as media

From the result, it obviously that the U-value decrease with the increase of the gap width, and with low emissivity coating of 0.065, the U-value is more acceptable than the high one. It is better to keep the low emissivity coating of 0.065 and control the width around 16-20 mm.

9. Solar collector for passive thermal comfort and water heating

9.1. Experimental set-up

The double glass window of area 0.5358(m²) with radiation reflective coating at inner pane has been tested experimentally at different angles. By measuring the water flow rate, inlet and outlet temperatures of the flow circuit across the glazed area, the useful heat gain of the system is determined. A radiation meter was installed parallel to the window/solar collector to record the incident solar radiations. The sensor signals (including thermocouples) were sent to a data logger and downloaded periodically for performance analysis. In this way, the system efficiency which is the ratio of useful heat gain to the water to the incident solar radiation on the glazing surface was evaluated.



Figure 39(a). Experimental setup.

The experimental set up for testing combined window/solar water heating collector is shown schematically in Figure.39 (a, b). It consists of a window/solar collector, water feeding tank, storage tank and a water circulating pump. The combined window solar collector is made up of two glass sheets of total dimensions of 0.94(m)x0.57(m) and effective area of 0.5358 (m²). The glass sheets are bound together with spacing of 5(mm) between them, their perimeter is sealed and the combined sheets are allocated within a metal frame hinged at its top side to two columns attached to a movable base for easy transport. The circulating water is fed at the bottom header from the water feed tank under static head and discharged at the top header to the storage tank. To ensure uniform water distribution in the spacing between sheets a fine screen is placed along both headers. The water circulating pump sucks water from the storage tank and supplies it to the top feed tank.

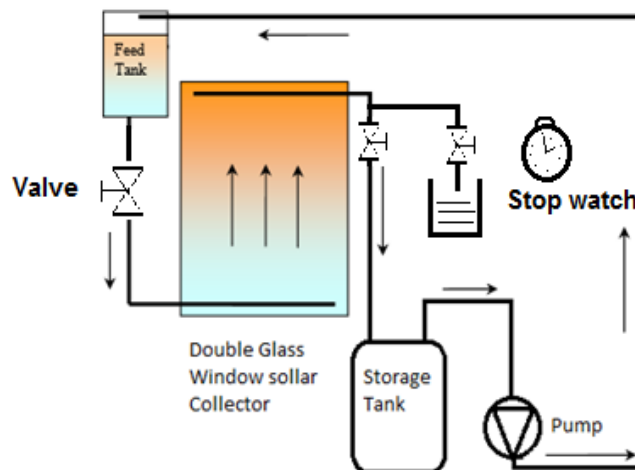


Figure 39(b). Schematic diagram of double glass window/Solar collector as a water heating device.

In order to evaluate the thermal performance of the collector, measurements of the temperature distribution along and over the front glass internal surface area were taken by calibrated thermocouples of the T type. The external surface area and the external surface temperature of the back glass sheet were also measured. Temperatures were also measured along the water flow direction between the glass sheets and at entry and exit of the combined window/solar collector.

The feed tank allows water to flow through the combined window/solar collector under gravity action. Its mass flow rate is measured by directing the water flow at the exit of combined window/solar collector to the mass measuring section as indicated in Figure.39 (a). After collecting a certain mass in a certain time the water is reverted back to the water circulation circuit. The wind velocity, the ambient temperature were also measured. The solar radiation is measured by an instrument placed at the same inclination of the com-

bined glass sheets. The detailed technical specifications of the collector, the thermal storage and measuring devices are listed in the table 8.

Table 8 Technical specification of the components and instruments

Design parameters and devices	Specifications
Tilt angles	0°,5°,10°,20°,35°,45°,55°,65°,75°,90°
Uncovered area of collector	0.5358 m ² (0.94×0.57)
Support	Aluminum
4 Thermocouples	T-Type
Radiation meter	Solar power meter MES-100
Field logger	Novus V 1.4
Storage tank	47(Liters)
Feed tank	11(Liters)

9.2. Test procedure

The procedure used in a typical test of the combined window/solar collector usually started by fixing the combined window/collector to the required inclination relative to the horizontal position and the radiation measuring instrument parallel to the surface of the window/collector. The valves fitted to the storage tank and the water feed tank are set to the operation position. All thermocouples are connected to the data acquisition system and the initial temperatures are registered. The pump is switched on and the reading of the radiation measuring instrument is registered. Water flow rate is measured after every 15 minutes and an average is considered as representative of one full day of testing. The tests usually continued for 5 hours daily. Wind velocity and ambient temperature were measured each hour. It is important to mention that the measurements were used to calculate the hourly average parameters by taking the hourly average of the measured parameters and the results are presented on an hourly basis as will be seen later.

This test procedure repeated for the following day after setting the combined window/solar collector to the new inclination each day. The inclination angles are presented in Table 8. It is important to mention that the inclination is varied since the window consequently the solar collector can take any angular position except 0° to the horizontal. In this position the glass sheets were damaged due to vapor formation and blockage due to stagnant conditions in the collector.

Uncertainty analysis of experimental measurements were performed for the mass flow rate, heat gain and temperature indicated by the thermocouple. The uncertainty found is presented in Table 9.

Table 9 presents the accuracy of various measuring devices used in the experiment

Parameters	Accuracy
Temperature difference (Thermocouple)	± 0.505 (°C)
Heat gain (Q)	± 6.15 to 11.06 (W)
Mass flow rate	$\pm 2.94e^{-4}$ to $3.47e^{-4}$ (kg/s)
Solar power meter	± 0.38 W/m ²
Tilt angle	$\pm 1^\circ$

9.3. Theoretical Analysis

In order to determine the efficiency parameters of solar thermal collectors, following equations were used.

T_{in} = Inlet temperature (°C)

T_{out} = Outlet temperature (°C)

$\Delta T = T_{out} - T_{in}$

η = Efficiency

I_o = Incident radiation (W/m²)

A = Area of glass window (m²)

\dot{m} = Mass flow rate (kg/s)

C_p = Specific heat of Water (Room Temp.)(J/kg.k)

Q_{out} = Energy out (W)

Q_{in} = Energy in (W)

In order to determine the efficiency of solar thermal collectors, two different procedures can be used: the steady state test and the quasi dynamic test method. During the steady state test, all boundary conditions such as incident solar irradiation, ambient temperature and inlet temperature of collector shall be maintained constant. In This technique, the basic idea is to expose the collector to solar radiation and measure the inlet and outlet temperatures of the working fluid flowing through it with a known flow rate. The heat rate gained by the fluid is then given by. (Duffie & Beckman, 2006)

$$Q_{out} = \dot{m}c_p\Delta T \quad (31)$$

The source of heat in a solar collector is solar energy and the input power is usually the incidence radiations, I_o , received on the surface of the collector, absorbed and then transferred to the working fluid.

$$Q_{in} = I_o A \quad (32)$$

By dividing the net energy output by the input energy, an overall efficiency can be defined. Such efficiency is considered as instantaneous efficiency because it is a function of instantaneous operating conditions such as the ambient temperature, the wind speed, etc.

$$\eta = \frac{Q_{out}}{Q_{in}} \quad (33)$$

10. RESULTS AND DISCUSSION

The experiments were conducted over a period of three months, from November to January, on a parking area located at Unicamp University Campinas. The experiments were conducted from 10.00 am to 03.00 pm.

The collector was tested at $0^\circ, 5^\circ, 15^\circ, 20^\circ, 35^\circ, 45^\circ, 55^\circ, 65^\circ, 75^\circ, 90^\circ$ angles at constant mass flow rate. All readings were taken periodically for performance analysis. After every 30 minutes the solar radiation values were measured by solar radiation meter.

10.1. Variation of ambient temperature and wind speed with time

The ambient temperature and wind speed varied throughout the test day. Both Parameters were not measured experimentally; however, the data were taken from an online source (weather.com). As seen in Figure 40, at the beginning of the test, the ambient temperature is low with a value of 20 , and it starts to increase as the time goes until it reaches a maximum value of 26.6 from 1:45 P.M to 3:15 P.M. Then, it decreases slightly at the end of the experiment. A minimum wind speed is found at 9:45 A.M with a value of 2.2 m/s. It starts to rise with time till it has the peak value 3.6 m/s from 1:45 P.M to 2:15 P.M.

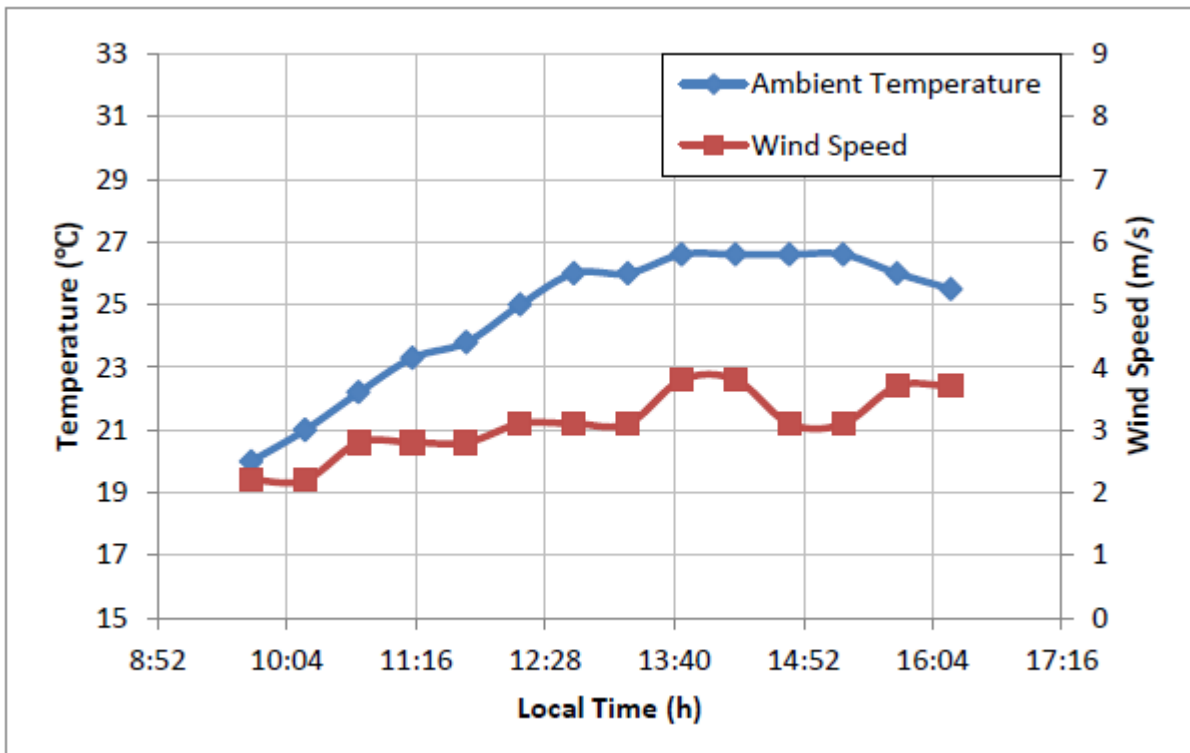


Figure 40: Variation of ambient temperature and wind speed with time

10.2. Obtained results at 90°

10.2.1. Radiations at 90°

The solar radiation were taken by fixing the solar radiation meter parallel to the face of solar collector

The graph plotted between solar intensity with time as shown in fig.41. The results indicates that the solar intensity increases with respect to time and maximum intensity 850 (w/m^2) was observed around 12:30 PM at angle 90° after that it has decreases with time due to low solar intensity.

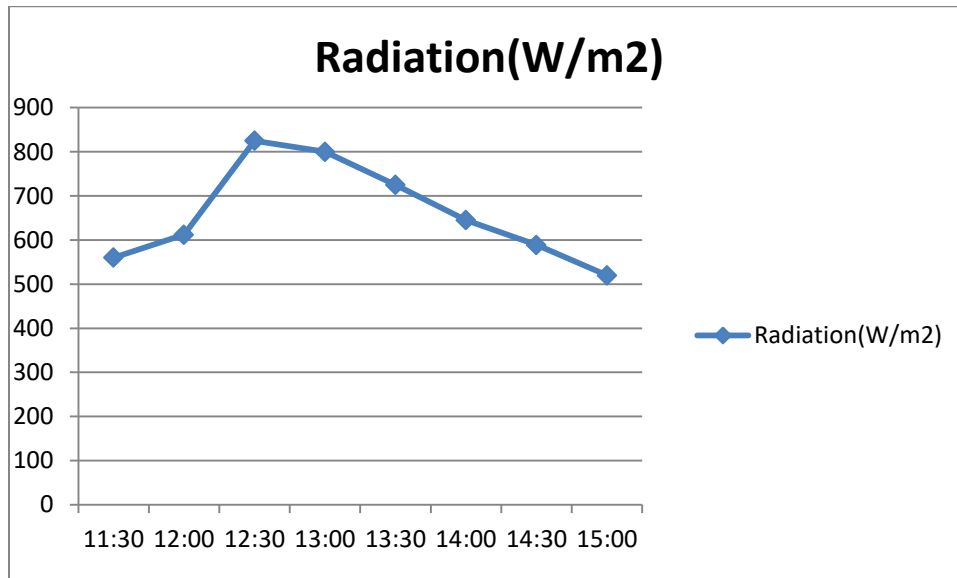


Figure 41. Variation of solar radiations during experimentation hours at 90°.

10.2.2. Variation of outlet and inlet temperature with respect to time

Figure.42 shows the variation of inlet temperature (T_{in}) and outlet temperature (T_{out}) respectively at an angle of 90° to the horizontal (when the window is in vertical position) during the experimentation hours. The outlet temperature was up to 40°C for the volume of 47L of water during 5 hours.

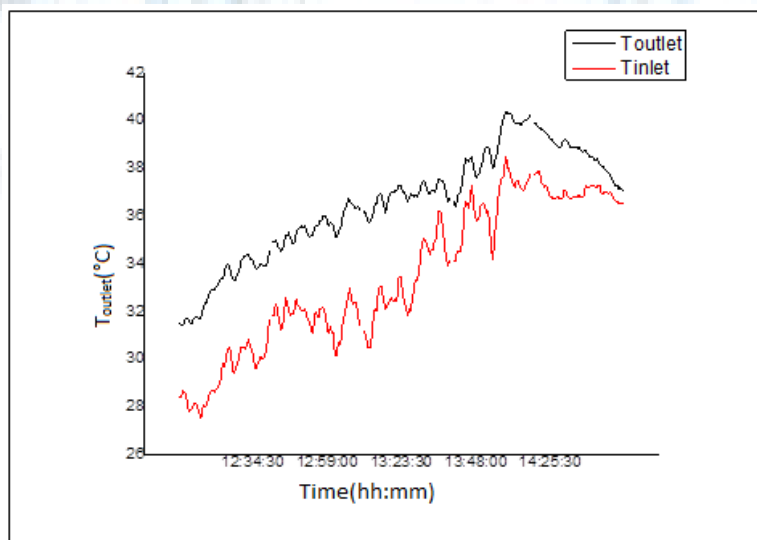


Figure 42. Variation of hot water outlet temperature during experimentation hours at 90°.

10.3. Obtained results at 0°

10.3.1. Radiations at 0°

The graph plotted between solar intensity with time as shown in fig.43. The results indicate that the solar intensity increases with respect to time and maximum intensity 1058 (w/m^2) was observed around 13:30 PM at angle 0° after that it has decreases with time due to low solar intensity.

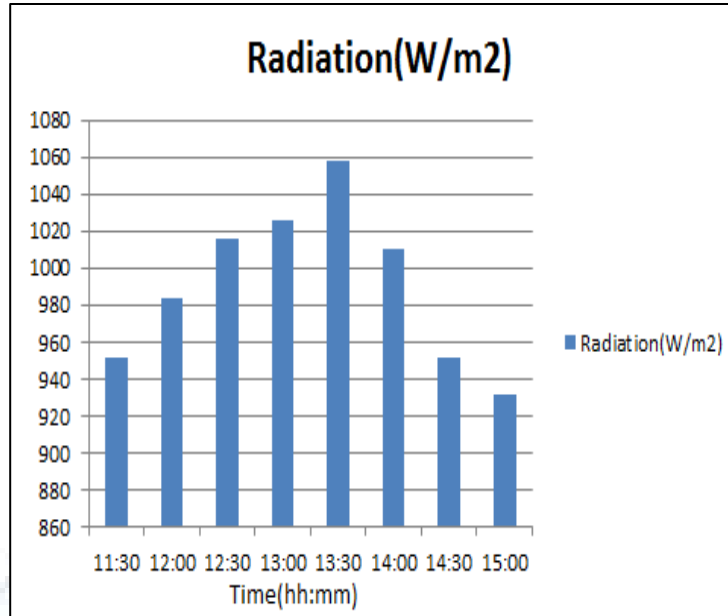


Figure 43. Variation of solar radiations during experimentation hours at 0°.

10.3.2. Variation of outlet and inlet temperature with respect to time

Figure 44. Shows the variation of inlet temperature (T_{in}) and outlet temperature (T_{out}) w.r.t time at an angle of 0°. It can be seen that at some points the inlet temperature is higher or equal to outlet temperature to due to vapor formation. It shows that window/collector can be used at any angular position except 0° to the horizontal.

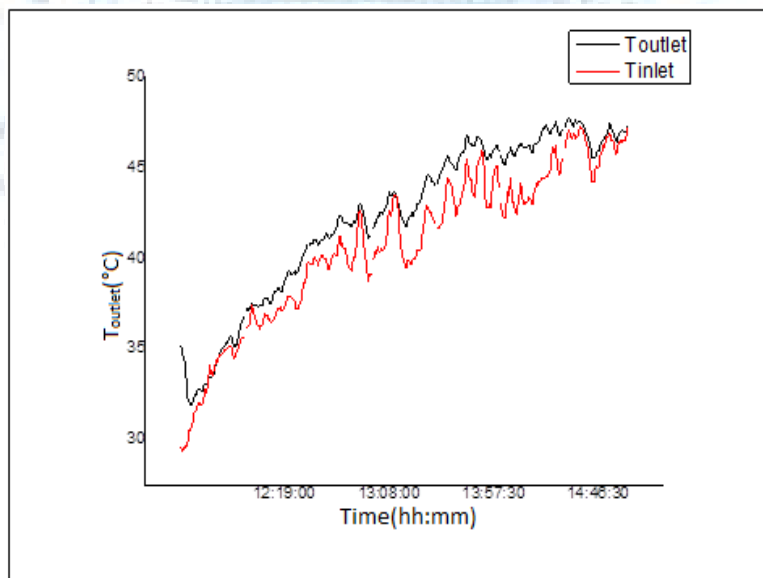


Figure 44. Variation of outlet and inlet temperature during experimentation hours at 0°.

10.4. Obtained results at 45°

10.4.1. Solar radiation

The graph plotted between solar intensity with time as shown in fig. 45. The results indicate that the solar intensity increases with respect to time and maximum intensity 850

(w/m^2) was observed around 12:30 PM at angle 45° after that it has decreases with time due to low solar intensity.

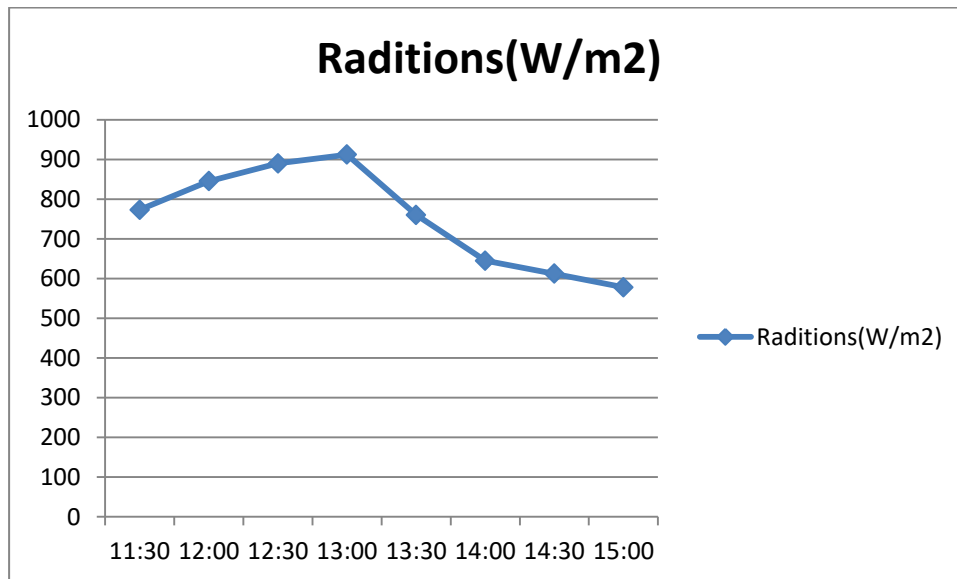


Figure 45. Variation of solar radiations during experimentation hours at 45° .

10.4.2. Variation of outlet and inlet temperature with respect to angles

Figure 46. Shows the average variation of inlet and outlet temperatures during experimentation hours with respect to angle. The maximum average outlet temperature recorded was 323 (k) at an angle of 45° degree. The average temperature difference ($T_{out} - T_{in}$) was about 7°C at an angle of 90° (which corresponds to the case of normal window position).

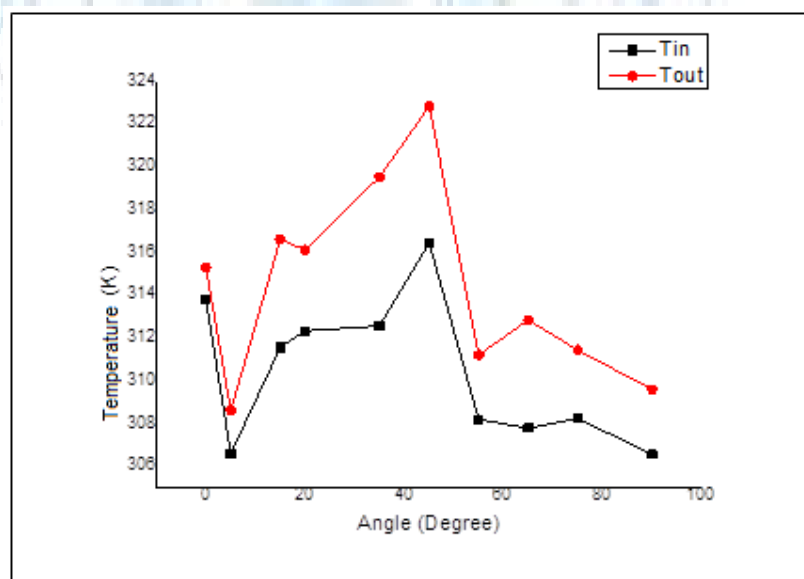


Figure 46 Variation of temperature at different angles

10.4.3. Useful heat gain (45°)

Figure 47. Show the variation of Q_{in} , Q_{out} and thermal efficiency w.r.t. angle. The efficiency of collector was higher between 45° angle to 65° angle. The thermal efficiency at angle of 90° (when the window is in vertical position) was 43%. Therefore, this novel window is an interesting alternative to conventional window in order to reduce solar gains, to protect the interior of the building, to reach significant heating, ventilation and air conditioning (HVAC) energy savings, and to take advantage of solar energy for commercial and domestic water heating.

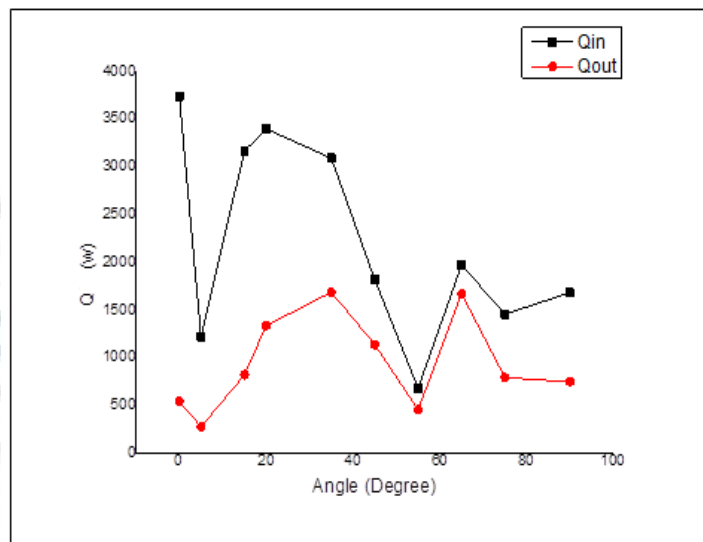


Figure 47. Variation of heat gain at different angles

Fig. 48 shows the efficiency of double glazing and spacing the collector with respect to angles so the effect of double glazing and spacing collector efficiency achieved was around 75% due to the higher heat gain.

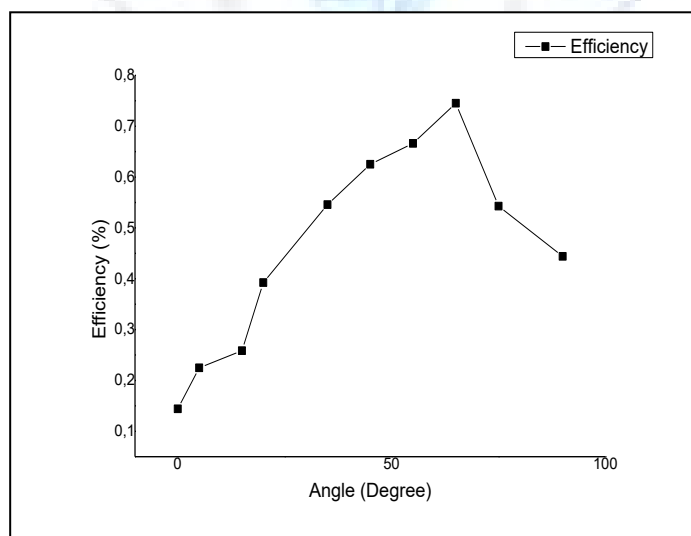


Figure 48. Variation of thermal efficiency at different angles

11. Conclusions

Field tests of the combined double glass window/ solar collector proved that the concept is feasible and can be used in domestic and commercial buildings for thermal comfort, architecturally more appealing and hot water generation. The presence of the reflective film seems to increase the heat gain while keeping the back side of the collector facing the room at relatively low temperature. The field tests showed variation of thermal efficiency of 45% to 67% at final temperature of 57(°C) during five working hours with collector area of 0.5358(m²).

12. References

- A.G. Hestnes, 1999. Building integration of solar energy systems, *Sol. Energy* 67 (46) (181e187)
- Chown, T., ChunyingLi, & ZhangLin. 2010. Innovative solar windows for cooling-demand climate. *Solar Energy Materials & Solar Cells*, 94, 212–220.
- Chow, T., Li, C., 2013. Liquid-filled solar glazing design for buoyant water-flow. *Building and Environment*, 60, 45-55.
- Duffie J.A., Beckman W., 2006. *Solar engineering of thermal processes*, 3rd ed., J. Wiley & Sons.
- Directive 2010/31/EU of the European Parliament and of the Council of 19 May 2010 on the Energy performance of Buildings, 2010
- D. Arasteh, H. Goudey, C. Kohler, 2008. Highly insulating glazing systems using nonstructural center glazing layers, in: *Proceedings of the Annual ASHRAE Meeting*, Salt Lake City, UT,
- Einasrud, M.A., Haereid, S., Wittwer, W. 1993. Some thermal and optical properties of a transparent Silica Xerogel material with low density. *Solar Energy Materials and Solar Cells*, 31, 334-347.
- Etzion, Y., Erell E. 2000. Controlling the transmission of radiant energy through windows: a novel ventilated Reversible glazing system. *Building and Environment*, 35, 433-444.
- Ismail, K.A.R, Henríquez, J.R. 2002. A parametric study on composite and PCM glass system. *Energy Conversion and Management*, 43, 973-993.
- Ismail, K.A.R., & Salinas, C. T. 2006. Non-gray radiative convective conductive modeling of heat transfer in double glass window with a cavity filled with mixtures of absorbing gases. *International Journal of Heat and Mass Transfer*, 49, 2972-2983.
- Ismail KAR, Salinas CT, Henriquez JG. 2008. Comparison between PCM filled glass windows and absorbing gas filled windows. *Energy Build*; 40:710–9.
- Onur N, Sivrioglu M, Turgut O. 1996. An experimental study on air window collector having a vertical blind for active solar heating. *Sol Energy*; 57:375–80.
- S.P. Corgnati, M. Perino, V. Serra, Experimental assessment of the performance of an active transparent façade during actual operating conditions, *Solar Energy* 81 (2007) 993–1013
- Tin-tai Chow, Chunying Li, J.A. Clarke. 2011. Numerical prediction of water-flow glazing performance with reflectiv coating , 12th Conference of International Building Performance Simulation Association, Sydney, 14-16 November. 1127-1131.
- U.S. Department of Energy (Ed.), *Buildings Energy Data Book*, D&R International Ltd., Silver Spring, MD, USA, 2009.)
- H. Manz, Numerical simulation of heat transfer by natural convection in cavities of facade elements, *Energy and Buildings* 35 (2003) 305–311.
- Weiss, W., Bergmann, I. e Faninger, G., *Solar Heat Worldwide – Markets and Contribution to the Energy Supply* 2004, IEA Solar Heating and Cooling Programme, 2006.
- Klein, S. A. e Beckman, W. A., *F-CHART User’s Manual (Windows Version)*, F-CHART Software, 2000.

European Database for Daylight and Solar Radiation, 2005. [online]:<http://www.satel-light.com/>.

Pereira, Enio B., Martins, Fernando R., Abreu, Samuel L. de, Ruther, R., Atlas brasileiro de energia solar, ISBN 978-85-17-00030-0. Sao Jose dos Campos – Brasil: INPE, 2006.

Atlas Solarimetrico do Brasil, Universidade Federal de Pernambuco, Companhia Hidroeletrica do Sao Francisco – 2001

Ceballos, J.C., M.J. Bottino, J.M. de Souza. A simplified physical model for assessing solar radiation over Brazil using GOES 8 visible imagery. *J. of Geophys. Research*, v. 109, D02211, doi:10.1029/2003JD003531, 2004.

Nair, M.T.S. and Nair, P.K. 1991, “SnS-CuxS Thin Film Combination: A Desirable Solar Control Coatings for Architectural and Automobile Glazing”. *Journal of Phys. D: Applied Phys.* 24: 450

Olesen, B.W. and Parsons, K. C. 2002, “Introduction to thermal comfort standards and to the proposed new version of EN ISO 7730”. *Energy and Buildings*, Volume 34, Issue 6.

Sengupta, J, Chapman, K.S. and Keshavarz, A. 2005a, “Window Performance for Human Thermal Comfort”. *ASHRAE Transactions*, 111 (1).

Sengupta, J, Chapman, K.S. and Keshavarz, A. 2005b, “Development of A Methodology to Incorporate Fenestration Systems into Occupant Thermal Comfort Calculations”. *ASHRAE Transactions*, 111 (1).

ASHRAE Standard 55-2004, Thermal Environmental Conditions for Human Occupancy, Atlanta: ASHRAE Inc.

Alvarez, G., Flores, J.J. and Estrada, C.A. 1998, “The Thermal Response of Laminated Glass with Solar Control Coating”. *J. Phys. D: Appl. Phys.* 31, 3057 – 3065.

Arasteh, D., Hartmann, J. and Rubin, M. 1987, “Experimental Verification of a Model of Heat Transfer through Windows”. *ASHRAE Transactions* 93, 1425 - 1431.

Bohm, M., Holmer, I., Nilsson, H. and Noren, O. 2002, Thermal Effect of Glazing in Driver’s Cabs, JTI-Report, Lantbruk & Industri 305, Uppsala, Sweden.

Hausler, T. and Beregr, U. 2002, “Determination of Thermal Comfort and Amount of Daylight”. *Air Conditioning, Air Protection & District Heating*, Szklarska Poreba, Juni 2002, Zusammenfassung.

Hawthorne, W. and Reilly, M.S. 2000, “The Impact of Glazing Selection on Residential Duct Design and Comfort”. *ASHRAE Transactions* 106 (1).

Karlson, T., Ribbing, C.G., Ross, A. and Valkonen, E. 1988, “Window Coating for efficient Energy Control”. *Int. J. Energy Res.* 12: 23 – 29

Lyons, P.R.A., Arasteh D. and Huizenga, C. 1999, “Window Performance for Human Thermal Comfort”. *ASHRAE Transactions* 73 (2), 4.0 – 4.20.

Schutrum, L.F., Stewart, J.L and Nevins, R.G. 1968, “A Subjective Evaluation of Effects of Solar Radiation and Raradiation from Windows on the Thermal Comfort of Women. *ASHRAE Transactions*, 74 (2), 115 – 128.

Estrada-Gasca, C.A., Alvarez-Garcia, G and Nair, P.K. 1993, “Theoretical Analysis of the Thermal Performance of Chemically Deposited Solar Control Coatings”. *J. Phys. D: Appl. Phys.* 26, 1304 - 1309.

Morton, W.E. and Hearle, J.W.S. 1993, 3rd edition, “Physical Properties of Testile Fibres”. The Textile Institute, UK

Tiwari G.N. Solar Energy. Fundamentals, Design, Modeling and Applications. – New Dehli: Alpha Science International Ltd, 2006. – p. 525.

Weiss W., Themessl A. Training Course – Solar Water Heating. Latvia – Baltic States. – Helsinki: Solpros AY, 1996. – p. 55.

Direct Thermal Conversion and Storage [online] [viewed 2007.11.25.]. Available:
www.osti.gov/accomplishments/pdf/DE06877213/10.pdf.

Yogi Goswami D., Kreith F., Kreider J.F. Principles of Solar Engineering. – New York: Taylor & Francis Group, 2000. – p. 694.

Duffie J.A., Beckman W.A. Solar Engineering of Thermal Processes. – New Jersey: John Wiley & Sons, Inc, 2006. – p. 908.

Ramlow B., Nusz B. Types of Solar Collectors [online] [viewed 2007.11.25.]. Available:
http://oikos.com/library/solarwaterheating/collector_types.html.

Rabl A. Active Solar Collectors and Their Applications. – New York: Oxford University Press, 1985. – pp. 503.

Gan, G. 2001, “Analysis of Mean Radiant Temperature and Thermal Comfort”. Building Serv. Eng. Research Technology 22.2: 95 – 101.

Ge, H. and Fazio, P. 2004, “Experimental Investigation of Cold Draft Induced by Two Different Types of Glazing Panels in Metal Curtain Walls”. Building and Environment 39, 115 – 125.

Chapman, K.S., Sengupta, J. 2004, “Window Performance for Human Thermal Comfort”.

Final Report of ASHRAE Research Project RP-1162, Atlanta: ASHRAE Inc.

Heiselberg, P. 1994. Draught risk from cold vertical surfaces, Building and Environment 29: 297-301. Indoor environmental technology paper n° 35 ISSN 0902-7531

Manz, H.; Frank, T. 2004. Analysis of thermal comfort near cold vertical surfaces by means of computational fluid dynamics, Indoor Built Environment 13: 233-242

John A. Duffie, William A. Beckman, “Solar engineering of thermal processes”, John Wiley and Sons, inc., 1991

Beckman, W. A., Solar Energy, **21**, 531 (1978). “Duct and Pipe Losses in Solar Energy Systems.”

Beckman, W. A., S. A. Klein, and J. A. Duffie, Solar Heating Design by the f-Chart Method, Wiley, New York (1977).

Collins, R.E., Simko, T.M., (1998), Current status of the science and technology of vacuum glazing, *Solar energy*, Vol. 62, Issue 3, pp. 189–213

ASTM (1991) Standard procedures for determining the steady state thermal transmittance of fenestration systems, ASTM Standard E 1423-91. Annual Book of ASTM Standards 04.07. American Society of Testing and Materials, pp. 1160–1165.

Djongyang, N., Tchinda, R., Njomo, D. (2010), Thermal comfort: A review paper, Renewable and Sustainable Energy Reviews, Vol. 14, Issue 9, pp. 2626–2640

Fanger, P.O., (1970), Thermal comfort, analysis and application in environmental engineering Danish Technical Press, Copenhagen

Gustavsen, A., Grynning, S., Arasteh, D., Jelle, B.P., Goudey, H.(2011), Key elements of and material performance targets for highly insulating window frames , *Energy and Buildings* , vol.43, Issue 10, pp.2583–2594

Reilly, M.S., Arasteh, D., Rubin, M., (1990), the effects of infrared absorbing gasses on window heating transfer: A comparison of theory and experiment. *Solar energy material* 20, pp. 277-288

Songa, S.Y., Job, J.H., Yeob, M.S., Kimb, Y.D., Songc, K.D. (2007), Evaluation of inside surface condensation in double glazing window system with insulation spacer: A case study of residential complex, *Building and environment*, vol.42, Issue 2, pp.940–950

<https://www.wychavon.gov.uk/documents/10586/157693/wdc-planning-her-windowsleaflet1.pdf>

http://www.ggf.org.uk/assets/0134-GGF_Window_Film_-_web-5053374e4372b.pdf

http://www.johnsonwindowfilms.com/dealer/documents/Film_to_Glass_Risk_Chart.pdf

